

LIFE-STAGE-SPECIFIC HABITAT ASSOCIATIONS AND DETECTION PATTERNS OF
PĀKU'IKU'I (*ACANTHURUS ACHILLES*) ON HAWAI'I ISLAND REEFS

PRESENTED TO THE FACULTY OF THE
TROPICAL CONSERVATION BIOLOGY AND ENVIRONMENTAL SCIENCE
GRADUATE PROGRAM

UNIVERSITY OF HAWAI'I AT HILO

HILO, HAWAI'I

IN PARTIAL FULFILLMENT OF THE REQUIREMENT FOR THE DEGREE OF
MASTER OF SCIENCE

IN

TROPICAL CONSERVATION BIOLOGY AND ENVIRONMENTAL SCIENCE

DECEMBER 2025

By: Annie Larson

Thesis Committee:

Lillian Tuttle Raz, Chair

Timothy Grabowski

Christopher Teague

Keywords: occupancy modeling, reef fish monitoring, detection probability, multi-method
surveys, Hawai'i nearshore fisheries

Acknowledgments

I am deeply grateful to my graduate committee for their guidance, support, and dedication throughout my master's journey. Dr. Lillian Tuttle Raz has been a remarkable advisor and mentor whose steady encouragement, thoughtful feedback, and generosity with her time were invaluable to this research. Dr. Tim Grabowski has been an incredible support throughout this project, especially in shaping the survey design, guiding the occupancy modeling, and helping to interpret the data. Christopher Teague has been a huge help, providing information from DAR and their developing understanding of *A. achilles* populations. Akaraporn Blaies provided invaluable diving support and was instrumental in completing the fieldwork. Additional thanks to Anthony White and Blue Robotics, who generously loaned us a BlueROV2 to complete our surveys, as well as Diego Johansen for making this connection. A special thanks to Dawn McSwain and Matthew Connelly for captaining the boat on many fieldwork days, as well as Samuel Chiu for providing ROV tether support. I would not have been able to complete this project without everyone's assistance.

I appreciate my parents, Troy and Tavia Larson, for always encouraging my passion for conservation and supporting me throughout my education. I also thank my partner, James Letuli, for motivating me to pursue another degree, listening to hours of practice presentations, and providing countless pep talks along the way. Additional thanks go to my colleagues at the Hawai'i Cooperative Fishery Research Unit, my TCBES cohort, the TCBES faculty, and the UH Hilo Marine Science Department. I would not have made it through this journey without the unwavering support and belief from my family, friends, and colleagues.

I also thank those who provided financial support for this work, including the Hawai'i Department of Aquatic Resources, Pacific Islands Climate Adaptation Science Center, and the

U.S. Fish and Wildlife Service through the U.S. Geological Survey's Cooperative Fishery Research Units program (contract no. G23AC00263). The Hawai'i Cooperative Fishery Research Unit is jointly sponsored by the U.S. Geological Survey, the University of Hawai'i System, the Hawai'i Department of Land and Natural Resources, and the U.S. Fish and Wildlife Service. I am sincerely grateful for this collective support, which enabled me to carry out and complete this research.

TABLE OF CONTENTS

Acknowledgments.....	ii
Table of Contents.....	iv
List of Tables.....	viii
List of Figures.....	ix
Abstract.....	x
1. Introduction.....	1
2. Methods.....	6
2.1 Study Area.....	6
2.2 Species Surveys.....	8
2.3 Environmental Drivers.....	11
2.4 Detection and Occupancy Modeling.....	15
2.5 Model Validation.....	20
3. Results.....	22
3.1 Patterns of Occupancy by Life Stage.....	22
3.2 Two-Species Detection-Occupancy Model Results.....	27
3.3 Detection Probability by Survey Method and Substrate.....	29
3.4 Model Validation.....	31
4. Discussion.....	31
4.1 Ontogenetic patterns of occupancy and life-stage connectivity.....	31
4.2 Detection and methodological implications.....	32

4.3 Management relevance, limitations, and future directions.....	36
Appendix.....	40
Table 1. Classification thresholds (mean \pm 1 SD) for depth, coral cover, and rugosity used in habitat stratification.	
Table 2. Linear regression results used to estimate missing site values for depth and coral cover from 25 m GIS covariates.	
Table 3. Linear regression results used to estimate missing site values for depth and coral cover from 100 m GIS covariates.	
Figure 1. Spearman rank correlation matrices for site-level occupancy covariates at 25 m and 100 m spatial resolutions.	
Figure 2. Principal Component Analysis (PCA) biplots of site-level occupancy covariates at 25 m and 100 m spatial resolutions.	
Table 4. Cross-scale habitat occupancy model comparison for the “All” dataset.	
Table 5. Cross-scale habitat occupancy model comparison for the “Juveniles” dataset.	
Table 6. Cross-scale habitat model comparison for “Adults” dataset.	
Table 7. <i>A priori</i> detection-only model set evaluating covariates influencing detectability across life stages.	
Table 8. Model-averaged parameter estimates from the single-season, two-species occupancy model for juvenile and adult pāku‘iku‘i.	
Table 9. Single-season occupancy model results for the “All” dataset ranked by AIC _c .	
Table 10. Single-season occupancy model results for the “Juveniles” dataset ranked by AIC _c .	

Table 11. Single-season occupancy model results for the “Adults” dataset ranked by AIC_c .

Table 12. Model-averaged β coefficients for detection and occupancy parameters from the “All” dataset.

Table 13. Model-averaged β coefficients for detection and occupancy parameters from the “Juveniles” dataset.

Table 14. Model-averaged β coefficients for detection and occupancy parameters from the “Adults” dataset.

Figure 3. Detection probabilities for juvenile and adult pāku‘iku‘i under different conditional states.

Table 15. Detection rate estimates from the single-season, single-species multi-method detection model for all life stages, juvenile and adult pāku‘iku‘i.

Table 16. Logistic regression coefficients describing detection probability as a function of unconsolidated substrate and survey method across life stages.

Table 17. Logistic regression slope estimates describing the relationship between detection probability and unconsolidated substrate across life stages and survey methods.

Figure 4. Predicted detection probability as a function of percent unconsolidated substrate for diver and ROV surveys across life stages.

Table 18. Predicted occupancy and detection validation results for pāku‘iku‘i at NOAA CREP survey sites around Hawai‘i Isla

Table 19. Summary of predicted detection–occupancy probabilities at NOAA CREP sites with observed and absent pāku‘iku‘i.

Figure 5. Comparison of predicted detection–occupancy probabilities between sites with observed and absent pāku‘iku‘i in the NOAA CREP dataset.

References.....84

LIST OF TABLES

Table 1. Variables used in occupancy and detection models, including descriptions and data sources.....	13
Table 2. Candidate occupancy models across life stages with AIC_c and model weights.....	23

LIST OF FIGURES

Figure 1. Study area and survey locations around Hawai'i Island.....	10
Figure 2. Relative variable importance across life stages.....	25
Figure 3. Model-averaged coefficient estimates for occupancy across predictors and life stages.....	26
Figure 4. Occupancy and detection probabilities across life stages and methods.....	30

ABSTRACT

Monitoring coral reef fishes is essential for assessing ecosystem health and managing fisheries, yet it remains challenging due to imperfect detection, complex habitats, shifting environmental conditions, and life-stage-specific behaviors. Detection–occupancy models address these limitations by separating detection probability from true occupancy. This study applied a single-season, multi-method (diver vs. remotely operated vehicle, ROV) single- and two-species (juvenile vs. adult) detection–occupancy framework to pāku‘iku‘i (*Acanthurus achilles*), a culturally, ecologically, and economically important reef fish in both commercial and noncommercial fisheries experiencing population decline along the west coast of Hawai‘i Island. Fifty-two sites around Hawai‘i Island were surveyed 3–4 times using combinations of SCUBA, snorkel, and ROV methods, and models incorporated environmental covariates representing human, oceanographic, and habitat conditions. Juveniles showed stronger associations with habitat conditions, including coral cover and relative slope, whereas adult occupancy was linked to broader oceanographic and human-based gradients. Adults were more likely to occur at sites where juveniles were present, suggesting habitat connectivity across life stages. Detection probabilities were comparable between survey methods, indicating that integrating ROV surveys may enhance monitoring efficiency and spatial coverage. Collectively, these findings demonstrate that accounting for imperfect detection improves inference about population status and habitat relationships for species with cryptic or ontogenetically shifting behavior. By modeling key habitat drivers and highlighting co-occurrence between life stages, this study provides actionable insight and a scalable framework to support recovery planning and adaptive management for an imperiled species on Hawai‘i’s nearshore reefs.

1. INTRODUCTION

Monitoring coral reef fishes is essential for assessing reef health, managing fisheries, and informing conservation decisions, yet it presents numerous technical and ecological challenges. Estimating abundance and distribution is difficult due to the cryptic behavior of many species (MacKenzie et al. 2006; Williams et al. 2006; MacNeil et al. 2010), complex habitat structures (Green et al. 2013; Suarez and Grabowski 2021), small fish size (Green et al. 2013), as well as fish responses to divers (Lindfield et al. 2014; Gray et al. 2016), habitat type (Suarez and Grabowski 2021), survey conditions (Williams et al. 2006), and observer experience (Williams et al. 2006), all of which can influence detection rates and lead to biased population estimates. These difficulties are especially pronounced for species that occur at low densities, shift habitats across life stages, or actively avoid divers (MacKenzie et al. 2006; Harford et al. 2016; Gray et al. 2016). Traditional survey methods also assume perfect detection and unbiased sampling across time and space, which are unlikely to be met under field conditions and only rarely assessed (Sequeira et al. 2018). Addressing these limitations requires approaches that account for imperfect detection and variability in survey performance across habitats and life stages.

To address these challenges, monitoring programs increasingly use multi-method survey designs and occupancy models that account for imperfect detection (Nichols et al. 2008). Combining different survey methods – such as diver surveys, underwater cameras, and fish traps – can increase the odds of accurately representing species presence and provide complementary information on habitat use across life stages so long as the differences in detection probabilities of the survey methods can be accounted for (Smith et al. 2006; Nichols et al. 2008). While many multi-method designs target multiple species within a taxonomic group (Manley et al. 2004; O’Connell et al. 2006), others focus on different size classes or life stages within a single species

(Smith et al. 2006; Mattfeldt and Grant 2007; Nichols et al. 2008). For example, combining transect and litterbag methods improved detection and occupancy estimates for cryptic salamander life stages (Mattfeldt & Grant 2007; Nichols et al. 2008), and detection of red snapper in reef habitats doubled when fish traps were paired with underwater cameras, allowing more accurate estimation of distribution and abundance (Coggins et al. 2014). These studies underscore the value of integrating multiple detection tools within an occupancy modeling framework to improve ecological inference and reduce bias in population assessments.

Detection–occupancy models distinguish the probability that a species occupies a site (ψ) from the probability that it is detected (p) when present (MacKenzie et al. 2002). This framework accommodates covariates that influence either process – such as observer experience or survey effort – or habitat complexity, by modeling how these factors affect detection or occupancy, ultimately reducing biases. By accounting for detection probabilities, occupancy models help avoid underestimating species presence, especially for rare, cryptic, or highly mobile species (Bacheler et al. 2014). In coral reef ecosystems, where structural complexity and species behavior strongly influence detection, such models have become increasingly important. For example, a recent study in Hawai‘i applied occupancy models to more than 500 coral-reef fish species across the Pacific Islands, showing that accounting for imperfect detection changed biomass estimates and could be applied to improve stock assessments (Suarez and Grabowski 2021). Similarly, Harford et al. (2016) identified habitat drivers of juvenile grouper distributions in Florida, highlighting the utility of this approach for linking species occurrence to environmental gradients. Collectively, these studies demonstrate the growing value of occupancy models in refining ecological inferences from survey data, particularly when detection varies among species, life stages, and habitats. However, applying occupancy models in reef

ecosystems requires repeated visits to each site to estimate detection, which increases the time and cost of diver-based surveys and can limit spatial coverage, which is problematic in heterogeneous habitats such as coral reefs. This limitation is particularly relevant for species that are patchily distributed or occupy complex terrain. These constraints highlight the potential value of complementary tools, such as ROVs, that can expand spatial coverage. ROVs can survey deeper or higher-energy habitats that are difficult or unsafe for divers to access, providing broader and more consistent coverage of heterogeneous reef environments.

These methodological advances are especially relevant for reef fishes that are both ecologically and culturally significant yet difficult to monitor reliably, such as the Achilles Tang (*Acanthurus achilles*), hereafter referred to by its Hawaiian name, pāku‘iku‘i. Pāku‘iku‘i are widely distributed across the tropical and subtropical Pacific, including Hawai‘i, French Polynesia, Micronesia, and the eastern Pacific (Randall 2001, 2007; Hoover 2008). This surgeonfish (Acanthuridae) is notable for its striking coloration and dual importance as a food and ornamental species. Its life history and habitat preferences make it a strong candidate for a multi-method occupancy modeling approach; juveniles are small and cryptic, often inhabiting deeper or more structurally complex reefs, whereas adults occupy high-surge shallow habitats that are challenging to survey safely (Randall 2007; Hoover 2008; DAR unpubl. data). These contrasting patterns across life stages create high potential for under-detection in conventional visual surveys.

Historically, pāku‘iku‘i was among the most frequently collected species in Hawai‘i’s commercial marine aquarium fishery, which primarily targeted juveniles (Tissot & Hallacher 2003), while adults were harvested for food in the noncommercial reef fishery, especially on Hawai‘i Island. Long-term monitoring by the Hawai‘i Department of Land and Natural

Resources (DLNR) Division of Aquatic Resources (DAR) between 2008 – 2020 documented marked declines in observed pāku‘iku‘i biomass and density on the island’s western (leeward) coast (hereafter “West Hawai‘i”), with adult biomass decreasing eightfold, density decreasing fourfold, and mean total length (TL) declining by approximately 3 cm (DAR unpubl. data). Juveniles were rarely observed in DAR surveys, with only 62 individuals recorded across two decades of surveys (1999–2021), but it was unclear whether this reflected true scarcity, low detectability, or the survey design not adequately capturing habitats favored by juveniles, as standard surveys were not specifically directed toward areas with higher juvenile potential. These species traits underscore the possible utility of implementing multi-method survey approaches that account for imperfect detection and provide more reliable, life stage-specific population assessments.

Recognizing these uncertainties, the Hawai‘i DAR implemented a two-year moratorium in December 2022 prohibiting both commercial and noncommercial harvest of pāku‘iku‘i in West Hawai‘i, later extended through 2026 (HAR §13-60.41). This closure was intended to facilitate research on the species’ biology and the drivers of its decline. Local initiatives, such as the Miloli‘i Community-Based Subsistence Fishing Area (CBSFA), had already established rest areas for pāku‘iku‘i prior to the shutdown of the West Hawai‘i aquarium fishery in 2017, when permits were no longer issued. However, the lack of apparent recovery following these closures suggests that overharvest alone may not explain observed trends. Additional factors such as recruitment limitation, habitat degradation, or detection bias may also contribute to the decline and continued low abundance of the species.

Despite the species’ importance, major gaps persist in understanding pāku‘iku‘i early life history and habitat connectivity. Juveniles are seldom encountered in surveys, and settlement

processes, dispersal, and migration patterns remain poorly documented. Observations (Randall 2001, 2007) and back calculations from settlement marks on otoliths (J. Honea unpubl. data) suggest that pāku‘iku‘i larvae settle at larger sizes (7–8 cm TL) than other surgeonfish and reach sexual maturity within 1–2 years (Grabowski et al. 2025). The combination of large settlement sizes and rapid growth may result in a low detectability of juvenile stages due to the limited amount of time individuals may persist in these stages. Adults are territorial grazers that inhabit high-energy shallow reefs (<5 m) and may form pairs or small aggregations when spawning year-round, although their reproductive behavior is not fully characterized (Randall 2007; Hoover 2008; Grabowski et al. 2025). Recent statewide modeling shows that pāku‘iku‘i presence is driven largely by habitat conditions, especially depth and rugosity, but the study’s presence–absence dataset limits its ability to determine whether the scarcity of juveniles reflects true rarity or low detectability (Layko & Donovan 2024). Collectively, these traits complicate monitoring and management, reinforcing the need for methods that can distinguish true absences from non-detection and improve inference about life stage-specific habitat use.

This study examines the ecology and distribution of pāku‘iku‘i across life stages around Hawai‘i Island using a single-season, multi-method detection and occupancy modeling framework. The species’ consistent absence from survey data suggests three possible explanations: they may be truly absent, they may be present in areas outside typical monitoring efforts, or they may be present but go undetected because of low visibility, diver avoidance, or other biases. Standard surveys cannot distinguish among these explanations, highlighting the need for approaches that explicitly model detection probability. Here, repeated SCUBA, snorkel, and remotely operated vehicle (ROV) surveys were combined with environmental covariates describing human, oceanographic, and habitat drivers to model both detection and occupancy

probabilities. This framework separates low abundance from detection bias and habitat-driven absence, improving inference on habitat relationships, life-stage distribution, and the effectiveness of survey methods for reef fish monitoring.

2. METHODS

2.1 Study Area

Hawai‘i Island (19.5° N, 155.5° W) is the largest, geologically youngest, and easternmost island in the Hawaiian Archipelago. The study area spans large nearshore regions of the island, encompassing a range of environmental conditions (Figure 1, Appendix Table 1). The island’s windward, eastern coastline (hereafter East Hawai‘i) exposed to prevailing trade winds experiences high rainfall and strong wave action, particularly during winter. The island’s southern coastline represents a transitional zone, characterized by moderate rainfall, high wind exposure, strong currents, and steep, rugged coastlines. These regions also differ markedly in depth, rugosity, and coral cover, creating strong habitat gradients around the island. In contrast, the leeward, western coastline (hereafter West Hawai‘i) has relatively calm seas, clear water, and the island’s and region’s most extensive coral reefs, despite major loss of coral cover during the bleaching event of 2015 (Hawai‘i Department of Land and Natural Resources 2019), contributing to strong island-wide gradients that provide relevant environmental context for identifying the habitat variables examined in this study.

Depth, rugosity, and live coral cover were hypothesized to be key variables influencing species distribution. Because juveniles were anecdotally observed more frequently in East

Hawai‘i than in West Hawai‘i, preliminary surveys were conducted in East Hawai‘i to explore potential drivers of their occurrence and to identify the most relevant habitat variables. Pre-existing, spatially explicit benthic data (2-m spatial resolution for depth and coral cover, and 6-m resolution for rugosity) across most of Hawai‘i Island (Asner et al. 2020, 2022) were used to develop an island-wide habitat map in ArcGIS Pro 3.1.0 (Esri 2023). Although rugosity was provided at a 6-m resolution, each pixel reflects structural complexity summarized over a 54-m square window centered on the pixel. These layers were aggregated within a 25×25 m grid to match the spatial scale relevant to pāku‘iku‘i habitat use, as preliminary observations suggest individuals occupy relatively small and localized foraging areas. No study has quantified pāku‘iku‘i home range, but published estimates for other surgeonfishes are substantially larger, for example *Naso unicornis* has a mean home range of 3,717 m² in Hawai‘i (Meyer and Holland 2005), and many reef fishes including surgeonfishes exhibit linear activity spaces ranging from 0.1 to 2 km (Meyer et al. 2010). Because pāku‘iku‘i appear more strongly territorial than these wide-ranging species, a smaller grid cell size was selected to better represent the spatial scale of their habitat use. Habitat categories for different combinations of relative depth, live coral cover, and rugosity (low, medium, and high for each) were defined using thresholds based on the mean \pm 1 SD of each variable relative to island-wide values (Appendix Table 1). For depth, low was classified as (0–7.44 m), medium as (7.45–14.178 m), and high (14.179–38.428 m). Coral cover was classified as low (0.001–7.7937%), medium (7.938–24.847%), and high (24.848–88%). Rugosity was classified as low (0–0.3294), medium (0.3295–0.6627), and high (0.6628–1). Only map-grid cells with at least five adjacent cells of the same category were considered suitable as candidate study sites to improve representative sampling across habitat types within each survey. A stratified random design was used to select 52 sites that evenly represented combinations of

the focal habitat variables and were distributed around the island to capture the range of nearshore conditions. Sites were clustered in areas that provided the greatest habitat variability within close proximity to accessible boat ramps. Site selection included areas with existing habitat data (Asner et al. 2020, 2022) and deeper regions beyond the extent of these datasets, while excluding the northeast and southeast coasts due to issues of access being either hazardous or lacking, and presumably limited habitat variability in these coastal stretches.

2.2 Species Surveys

Survey design was based on a two-method detection–occupancy framework (MacKenzie et al. 2002). All sites were surveyed 3–4 times using divers (SCUBA or snorkel), ROV, or a combination of methods depending on a site’s relative depth, safety, and accessibility. SCUBA surveys were limited to approximately 18.0 m due to depth and safety considerations, while snorkel was used at sites shallower than 4.6 m. ROVs were used at all other sites, except where shore access made deployment unsafe or impractical without a boat. All replicate surveys for any given site were completed within four weeks, and the full survey period spanned July through October 2024.

At SCUBA sites, one diver deployed a 25-m transect line and filmed the benthos using an underwater video camera (GoPro HERO13; GoPro, Inc. 2024) oriented perpendicular to the seafloor, while a second diver swam approximately 1 m above the other diver, recording all pāku‘iku‘i within 2 m of the transect (4 m wide belt). Individuals were categorized as adult or non-adult (juveniles or recruits) based on coloration, morphology, and visually estimated size (recruits ≤ 7 cm TL, juveniles > 7 cm TL and ≤ 13 cm TL, adults > 13 cm TL; DAR unpubl. data). The team then returned to the survey starting position, rotated at least 90° from the initial

heading, and conducted a second transect within a similar depth range and habitat type. Each transect lasted five minutes, for an approximately 10-min total survey time. Snorkel surveys were used in shallow habitats (<3 m), following a modified version of the SCUBA methods whereby snorkelers swam side-by-side at the surface, rather than one above the other.

A BlueROV2 Heavy Configuration ROV (BlueRobotics, Torrance, California) using QGround Control software v. 4.4.0 (Dronocode Project, Inc., 2024) software was deployed for ROV surveys. In addition to the onboard, front-facing camera, a HERO13 action camera (GoPro, Inc., San Mateo, California) was mounted in a front-facing position to the dorsal surface of the ROV to provide for higher resolution imagery. The ROV was piloted < 1 m above the seafloor in sequential passes that radiated out and back four times along the four cardinal directions to/from a survey centroid and lasting 8–10 minutes in total, with each pass covering approximately 10 m, estimated using surrounding benthic features and reference distances from divers who visited the same location. After the survey was completed and video footage downloaded, the action camera footage was used to identify pāku'iku'i and assign life history stage and size, which were visually estimated to nearest cm TL by the same experienced individual who sized fish during SCUBA and snorkel surveys for consistency. During both diver-based and ROV surveys, method (diver or ROV), depth, start time, and survey duration were recorded as detection model covariates.

Benthic habitat composition was assessed from video collected during diver-based and ROV surveys. Still frames were extracted at 10-s intervals using Gretech Online Movie Player (GOM; Gretech Corporation, Seoul, South Korea) and annotated in CoralNet (<https://coralnet.ucsd.edu>) with standardized substrate categories (live coral, dead coral, unconsolidated substrate, and non-coral hard bottom; Beijbom et al. 2012). Each image was

overlaid with a 4×3 grid for 12-point classification, yielding $\sim 10,000$ human-approved annotations; water points were excluded, and percent cover was calculated for each habitat category per survey. These values were used to ground-truth remotely sensed rasters in ArcGIS and as detection covariates to account for fine-scale substrate variability between survey events.

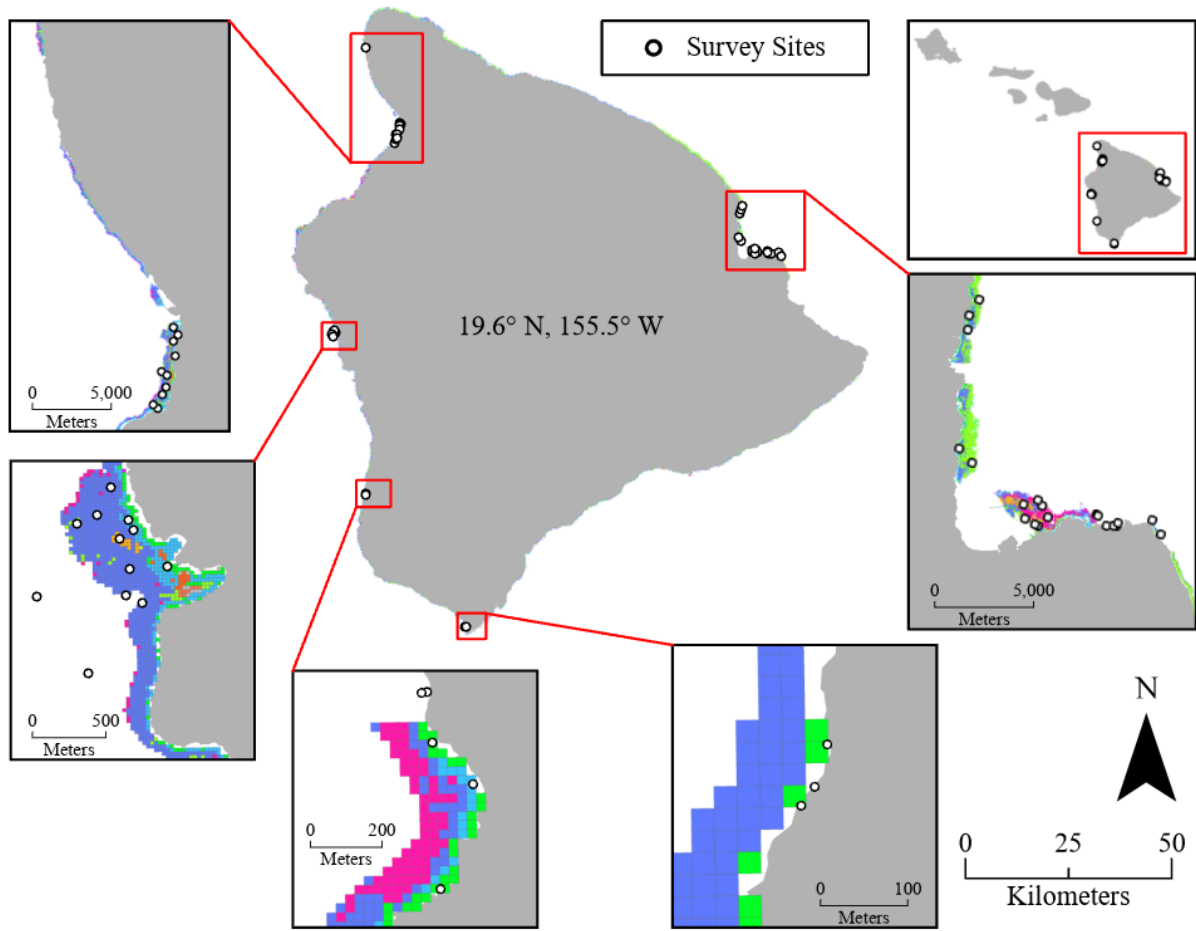


Figure 1. Survey sites ($n = 52$) around Hawai'i Island used to assess pāku'iku'i occupancy and detection using SCUBA, snorkel, or ROV methods between July-October 2024. Insets highlight focal regions in East and West Hawai'i. Colors indicate habitat categories for different combinations of relative depth, rugosity, and live coral cover (Appendix Table 1). Images derived from Hawai'i Statewide GIS Program 2022.

2.3 Environmental Drivers

Occupancy covariates (Table 1) included depth, coral cover, and rugosity from the Global Airborne Observatory (Asner et al. 2020, 2022) as well as depth range, calculated as the difference between the minimum and maximum depth within each 100 x 100 m grid cell. Additional variables, including total estimated average annual catch of reef fish (kg/ha), long-term mean wave power (kW/m), total effluent from onsite sewage disposal systems (gal/day/km²), annual amount of sediment (tons/yr/ha) export to nearshore waters, long-term mean sea surface temperature (°C), and chlorophyll-a average annual frequency of anomalies (fraction of a year) were sourced from the Ocean Tipping Points (OTP) Project, Hawai‘i Case Study (Wedding et al. 2018), hosted by the Pacific Islands Ocean Observing System (PacIOOS). These OTP variables reflect conditions extrapolated from data collected during 2000–2013 and are the highest resolution, spatially explicit data available to describe both human-based and oceanographic conditions around the Hawaiian Islands. The GAO publications do not provide specific reasons for missing values, but these gaps likely reflect incomplete spatial coverage resulting from flight-path restrictions and logistical constraints in mapping the entire nearshore coastline. Mean values for each survey site were extracted from the corresponding grid cell, with missing data estimated as follows. For coral cover and depth, missing mean values were estimated using linear regressions between *in situ* observations and GIS covariates (Appendix Tables 2,3) by subtracting the regression intercept from the mean *in situ* value of the missing site and then dividing the result by the slope. Because coral cover was missing for 16 of the 52 sites, a larger proportion than for any other habitat variable, these regression-based estimates likely introduce greater uncertainty into the coral-cover covariate. Although this approach allowed all sites to be retained in the analysis, the reliance on estimated values may affect the precision of coral cover’s effect size and its relative importance compared to predictors with complete spatial

coverage. As for depth range, this covariate required an additional shoreline-distance adjustment, which was calculated by subtracting the closest minimum GIS depth from the mean *in situ* value of the missing site and dividing that difference by the number of meters measured perpendicular to shore to the nearest available GIS depth value. Any missing sediment and effluent values were replaced with zeros, as sites distant from river mouths or discharge point sources were omitted from the OTP dataset. For rugosity, missing values were filled using the nearest available cell (4 sites <5m away, 1 site <275m away, 1 site <350m away). A Spearman correlation test and Principal Component Analysis (PCA) were conducted for occupancy variables at both 25-m and 100-m scales (Appendix Figures 1,2). No strong correlations ($|\rho| \geq 0.70$) or clear PCA clustering were observed, supporting flexible construction of candidate models without restricting variable combinations (Ali Abd Al-Hameed 2022). All occupancy predictors were then modeled at the 100×100 m scale, but coral cover, rugosity, mean depth, and depth range were each evaluated at both 25×25 m and 100×100 m resolutions. Cross-scale comparisons for the All, Juvenile, and Adult datasets (Appendix Tables 4–6) showed that only coral cover and rugosity performed better at 25 m, supporting the use of finer-resolution covariates for these two predictors.

Table 1. Variables for detection and occupancy models, including descriptions and data sources for each. Percent missing indicates the proportion of sites with missing data, calculated using alternative methods. Occupancy variables include depth, depth range, live coral cover, rugosity, sedimentation, effluent, fisheries catch, wave power, sea surface temperature and chlorophyll-a around Hawai‘i. Detection variables represent survey-level factors and include survey method, time of day, survey duration, substrate type, and survey depth.

Variables and Units	Description	Data Source	% Missing
Depth mean (m)	Empirical high-resolution benthic depth at a 2 m scale was derived from airborne imaging spectroscopy data collected by the GAO in January 2019 and 2020. Mean was calculated from all values in both 25 m and 100 m grid cells.	Asner et al. 2020 Global Airborne Observatory: Hawaiian Islands Bathymetry 2019+2020	3.846
Depth range (m)	Maximum depth was subtracted from minimum depth within the designated area.	Asner et al. 2020 Global Airborne Observatory: Hawaiian Islands Bathymetry 2019+2020	3.846
Live coral cover (%)	Empirical live coral distribution at a 2m scale to 16 m depth across the main Hawaiian Islands was derived from airborne imaging spectroscopy and deep learning data collected by the GAO in 2020.	Asner et al. 2022 Global Airborne Observatory: Hawaiian Islands Live Coral Cover 2020	30.77
Rugosity (m)	Empirical high-resolution seafloor rugosity at a 6 m scale was derived from airborne imaging spectroscopy data collected by the GAO in January 2019 and 2020.	Asner et al. 2020 Global Airborne Observatory: Hawaiian Islands Reef Rugosity 2019+2020	11.54
Sedimentation (tons/hectare/year)	Modeled sediment export to nearshore waters throughout the Hawaiian Islands.	Wedding et al. 2018 Ocean Tipping Points (OTP), Hawai‘i Case Study	38.46
Effluent (gallons/km ² /day)	Modeled total effluent from onsite sewage disposal systems in Main Hawaiian Islands. Units	Wedding et al. 2018	0

	are expressed as gallons per day per square kilometer. The area analyzed includes a 1 km stretch inland and extends 5 km offshore from the shorelines of the Main Hawaiian Islands.	Ocean Tipping Points (OTP), Hawai'i Case Study	
Fishing effort (kg/ha)	Modeled total estimated average annual catch of reef fish in Main Hawaiian Islands 2003-2013. Catch categories include non-commercial shore, non-commercial boat, and commercial, with fishing gear including line, net, and spear.	Wedding et al. 2018 Ocean Tipping Points (OTP), Hawai'i Case Study	0
Wave power (kW/m)	Modeled average annual frequency of wave power anomalies was determined by calculating the mean number of days per year that wave power exceeded the monthly climatological maximum 2000-2013, for each 500-meter grid cell.	Wedding et al. 2018 Ocean Tipping Points (OTP), Hawai'i Case Study	0
Sea surface temperature (°C)	Modeled long-term mean sea surface temperature (°C) from weekly composites 2000-2013	Wedding et al. 2018 Ocean Tipping Points (OTP), Hawai'i Case Study	0
Chlorophyll- <i>a</i> (yr fraction)	Modeled annual average number of chlorophyll- <i>a</i> anomalies (mg/m ³) 2002-2013.	Wedding et al. 2018 Ocean Tipping Points (OTP), Hawai'i Case Study	0
Survey method (categorical)	ROV, SCUBA, or snorkel (latter two combined into 'diver')	In-situ collected data	0
Time of day (categorical)	AM or PM	In-situ collected data	0
Survey duration (continuous)	In minutes, ranged from 10-14	In-situ collected data	0
Substrate type (categorical)	Raw video footage of benthic habitat from surveys uploaded to GOM, then classified in CoralNet, then percentages	In-situ collected data	0

	calculated in Microsoft Excel. Categories: live coral, dead coral, unconsolidated (sand, mud), non-coral hard bottom		
Survey depth (m)	Displayed on screen (ROV), or recorded during survey (SCUBA or snorkel)	In-situ collected data	0

2.4 Detection and Occupancy Modeling

Detection probability and site occupancy for pāku‘iku‘i were estimated using a single-season occupancy model and associated assumptions, as described by MacKenzie et al. (2018) and implemented using the *RPresence* package (MacKenzie & Hines 2023) in R 4.5.1 (R Core Team 2025). In the context of this framework, occupancy (ψ) can be interpreted both as the proportion of sites where pāku‘iku‘i is present and as the probability that pāku‘iku‘i is present at any given site. Detection (p) represents the probability of observing and recording pāku‘iku‘i at a site, given that it is present. Factors that remain constant across surveys (i.e., environmental drivers) were occupancy covariates, while factors that vary among surveys (i.e., survey method and *in situ* measurements derived from CoralNet) were detection covariates (Table 1). *In situ* measurements were included in the detection component of the model because detection probability can vary with fine-scale habitat features that are not captured by remotely sensed covariates. Local substrate composition, small patches of sand or rubble, and subtle differences in coral structure can affect both fish visibility and survey performance, and these conditions often differ among replicate surveys at the same site. Accounting for this within-site variation in benthic composition was especially important because no permanent markers were installed to ensure identical survey start points across repeat visits, meaning each pass could encounter

slightly different portions of the reef. Incorporating in situ observations therefore allowed the detection model to account for survey-specific benthic conditions and reduce bias in estimating true occupancy. In contrast, the coral cover used as an occupancy covariate was derived from the Global Airborne Observatory dataset and represents a static, site-level habitat condition that does not vary across repeated surveys. This differs fundamentally from the in situ coral cover estimates, which reflect the actual microhabitat encountered during each individual survey pass. Including both scales allowed the occupancy model to incorporate stable habitat features influencing true presence, while the detection model captured survey-level benthic conditions that influence detectability.

To identify the most appropriate detection covariates for the occupancy analysis, a set of detection-only models was first run with occupancy held constant (null). Twelve candidate detection models were evaluated across three model categories (“Juveniles” for recruits and juveniles only, “Adults” for reproductively mature adults only, and “All” for all life stages) (Appendix Table 7). The models were ranked using Akaike's Information Criteria for small sample sizes (AIC_c ; Akaike 1973; Burnham & Anderson 2004) with the model with the lowest AIC_c value considered the top model (Appendix Table 7). AIC_c is an information-theoretic criterion that evaluates the relative predictive performance of competing models rather than their absolute fit to the data. As emphasized by Burnham and Anderson (2004), models are treated as approximations to reality, and the goal of AIC_c -based selection is to identify the model that minimizes information loss rather than one that perfectly reproduces observed data. Similarly, Stewart et al. (2023) demonstrated that information criteria can select models that yield reliable predictions of occupancy even when fit is imperfect, provided the objective is to describe spatial patterns and identify influential predictors rather than to infer strict causal relationships. For each

life stage, only one detection model had $\Delta AIC_c \leq 2.0$, indicating no model selection uncertainty. The best-supported detection model, which was consistent across life stages, was then applied as the fixed detection parameterization for all subsequent occupancy models (Appendix Table 7).

All count data were first converted to binomial presence/absence data, with a value of 1 assigned when pāku‘iku‘i was detected in any survey at a site and 0 assigned when no detections occurred. Continuous occupancy and detection covariates were then standardized (z-score) prior to model fitting to improve model convergence and comparability of parameter estimates. Each variable was transformed to have a mean of zero and a standard deviation of one using:

$$z = (x-\mu)/\sigma \text{ [Equation 1]}$$

where x is the raw covariate value, μ is the mean, and σ is the standard deviation. Occupancy covariates were standardized across all sites, while detection covariates (e.g., percent unconsolidated substrate) were standardized across all site \times survey combinations.

When pāku‘iku‘i was not detected at a site ($y_i = 0$), the true occupancy (ψ_i) state was unknown and therefore expressed as a two-part conditional probability (MacKenzie et al. 2006): either the species is present ($\psi_i = 1$) but went undetected ($p_i < 1$), or it was absent ($\psi_i = 0$). This relationship is represented as:

$$p_{(y_i = 0)} = \psi_i(1 - p_i)^k + (1 - \psi_i) \text{ [Equation 2]}$$

When a species is detected ($y_i > 0$) in at least one survey (k), the detection history can be represented as a random binomial variable with an inflated zero class:

$$p_{(y_i > 0)} = \psi_i \binom{k}{y_i} p_i^{y_i} (1 - p_i)^{k-y_i} \text{ [Equation 3]}$$

Equation 3 outlines the core structure of detection–occupancy modeling for individual species but does not account for heterogeneity among sites. Such heterogeneity between sites and surveys can be explained by incorporating covariates (MacKenzie et al. 2002). Occupancy covariates (x) are site-specific and temporally constant, consistent with the assumption of a closed population, while detection covariates may vary across surveys. These covariates are incorporated into the model using a linear model with a logit link function:

$$\frac{\psi_i}{(1-\psi_i)} = \beta_0 + \beta_1 x_1 + \dots + \beta_j x_j + \varepsilon \text{ [Equation 4a]}$$

$$\frac{p_i}{(1-p_i)} = \gamma_0 + \gamma_1 x_1 + \dots + \gamma_j x_j + \varepsilon \text{ [Equation 4b]}$$

where parameters associated with occupancy covariates are denoted by β , while parameters associated with detection covariates are denoted by γ .

Occupancy models were developed and evaluated with detection and occupancy probability modeled as functions of environmental and human covariates defined *a priori* (Table 2) and implemented for the All, Juvenile, and Adult survey results separately. Candidate models were ranked using AIC_c , and models with $\Delta AIC_c < 6$ comprised the “confidence set” for multimodel inference. Model weights (w_i) were normalized within this set and used to calculate model-averaged estimates of β estimates for each covariate. Unconditional standard errors and 95%, 80%, and 50% confidence intervals were computed following Burnham and Anderson (2002) to account for model-selection uncertainty. Variable importance was quantified as the sum of AIC_c weights across all models containing a given covariate ($\sum w_i$). To reduce potential bias from correlated or redundant parameterizations, variable-importance values were further adjusted following Cade (2015), who recommends down-weighting importance scores when the same predictor appears in multiple, closely related model structures. In practice, this involves

scaling the summed weights by the number of distinct model parameterizations in which the variable appears, yielding an estimate that reflects the predictor's unique contribution rather than inflated support from highly similar models.

Next, a single-season, two-species occupancy model (MacKenzie et al. 2004) was used to evaluate the probability of detection and occupancy of juvenile and adult pāku'iku'i when the other 'species' (i.e., life stage) was present and detected. The model was parameterized with $psiBa/rBa$, where $psiBa$ is the probability that the area is occupied by adults given juveniles are present, and rBa is the probability of detecting adults given both life stages are present but juveniles were not detected. This parameterization allowed us to examine: 1) the probability that a site is occupied by adults when juveniles are present, and 2) the probability that a site is occupied by adults when juveniles are absent. Because the two-species parameterization includes eight default parameters, we did not include site- or survey-level covariates to avoid over-parameterization (Anderson 2008). We developed four *a priori* models that allowed detection probabilities to vary between life stages when present and detected (Table 3). To account for model uncertainty, model-averaged estimates of occupancy and detection probabilities were derived from the full set of *a priori* models following Burnham and Anderson (2002, 2004; Appendix Table 8).

Then, a single-season, single-species, multi-method detection model was developed to evaluate differences in detection probability between diver and ROV surveys across life stages ("All," "Juveniles," and "Adults"; Nichols et al. 2008). Detection was modeled as a function of survey method (diver vs. ROV), while occupancy was held constant as an intercept-only term ($\psi \sim 1$). One *a priori* model was implemented for each life stage, with detection allowed to vary between methods.

In addition to evaluating detection differences between survey methods, a single-season, single-species model was run in which occupancy was held constant (null) and detection probability was modeled as a function of survey method (diver vs. ROV) and percent unconsolidated substrate across the three life stage groupings (MacKenzie et al. 2002). This parameterization allowed examination of how increasing proportions of unconsolidated habitat influenced detection rates for divers and ROVs, with predicted detection probabilities generated from model-derived parameter estimates using the logistic function.

2.5 Model Validation

Models were validated using the National Oceanic and Atmospheric Administration (NOAA) Coral Reef Ecosystem Program (CREP) dataset, which represents the best publicly available, long-term reef fish monitoring data for Hawai‘i (Heenan et al. 2017; NOAA Coral Reef Ecosystem Program (CREP) (2025)). The NOAA-CREP Pacific Reef Assessment and Monitoring Program (RAMP) is a multi-disciplinary coral-reef monitoring program containing stationary point count (SPC) survey data of coral-reef fishes (Heenan et al. 2017), from which survey data collected during 2010–2016 were used for the validation process. SPC surveys consist of two divers conducting simultaneous counts in adjacent 15-m diameter cylinders. For consistency with our framework, these paired diver counts were treated as repeat surveys and combined into a single site-level record. The SPC design is spatially comparable to the transect-based methods used in this study in terms of the area searched, though it differs slightly in survey implementation.

We filtered the CREP dataset to pāku‘iku‘i presence–absence observations from 153 sites around Hawai‘i Island and extracted the same set of occupancy covariates at those locations

using the same datasets (Wedding et al. 2018; Asner et al. 2020, 2022) and following the same procedures described for our survey data. To maintain consistency in variable scaling, detection and occupancy covariates were standardized using the means and standard deviations from the training dataset. Predicted occupancy and detection probabilities for each CREP site were generated using the model-averaged logit equation from the “All” life-stage dataset, which combined juvenile and adult observations. Model-averaged coefficients were derived from the confidence set of models with $\Delta AICc < 6$. Detection probability was modeled as a function of survey method + percent unconsolidated substrate, consistent with the structure of all detection–occupancy models developed in this study. For sites with two diver replicates, the probability of detecting at least one pāku‘iku‘i individual was computed as:

$$P(\geq 1 \text{ detection}) = 1 - ([1 - (\psi \cdot p_1)] \times [1 - (\psi \cdot p_2)]) \text{ [Equation 5]}$$

To assess model discrimination, predicted detection–occupancy probabilities were compared between CREP sites where pāku‘iku‘i were observed and sites where they were absent using a Mann–Whitney U test (Wilcoxon rank-sum test; Wilcoxon 1945; Mann & Whitney 1947). This nonparametric test evaluated whether predicted probabilities were significantly higher at presence sites, providing a statistical measure of the model’s ability to distinguish occupied from unoccupied sites.

3. RESULTS

3.1 Patterns of Occupancy by Life Stage

A total of 19 candidate occupancy models were evaluated for each life stage (All individuals, Juveniles, and Adults), representing alternative combinations of human, habitat, and oceanographic predictors (Table 2). The overall goodness-of-fit ($\hat{c} = 0.45\text{--}0.84$) indicated mild underdispersion across life stages (Appendix Tables 9–11), but this level of dispersion does not raise concern for model inference, as corrections in occupancy models are typically only made for overdispersion.

Models with $\Delta\text{AIC}_c < 6$ accounted for most of the model weight in each life stage ($\sum w_i = 0.98, 0.93,$ and 0.94 , respectively), indicating moderate to strong support for a limited subset of models. For the “All” individuals dataset, the top-ranked model included both human and habitat predictors (fish catch, depth range, and coral cover; $w_i = 0.23$), followed by a habitat-only model containing depth range ($w_i = 0.21$) and a coral cover model ($w_i = 0.12$; Table 2). A mixed model including effluent, coral cover, and chlorophyll-*a* also received moderate support ($w_i = 0.16$; Table 2). For the “Juveniles” dataset, habitat variables dominated model performance. The best-supported model included coral cover alone ($w_i = 0.41$), followed by depth range ($w_i = 0.25$; Table 2). Mixed models combining human, habitat, and oceanographic predictors received lower but non-negligible support ($w_i \approx 0.11\text{--}0.13$; Table 2). For Adults, the top model incorporated effluent, coral cover, and chlorophyll-*a* ($w_i = 0.30$), followed by a mixed human–habitat model including fish catch, depth range, and coral cover ($w_i = 0.17$; Table 2). Habitat models containing depth range ($w_i = 0.14$) and oceanographic models with chlorophyll-*a* ($w_i = 0.10$) also ranked among the most supported (Table 2).

Table 2. Candidate single-season occupancy models for all individuals, juveniles, and adults. Models are grouped by category (Human, Oceanography, Habitat, Mixed, Null, and Global). Columns show the corrected Akaike Information Criterion (AIC_c), the difference in AIC_c relative to the best model (ΔAIC_c), and the Akaike model weight (w_i), which reflects the relative support for each model within a life stage. Rank shows the model's position when ordered by AIC_c . Darker shades indicate higher AIC_c weights ($w_i < 0.1$ = lightest, $w_i < 0.2$ medium, $w_i < 0.3$ dark, $w_i > 0.3$ darkest). **Bolded** values indicate models included in the confidence set ($\Delta AIC_c < 6$) used for model averaging. The sum of the model weights associated with the confidence set is represented as Σw_i .

Model Group	Occupancy Predictors	All $\Sigma w_i = 0.98$			Juveniles $\Sigma w_i = 0.93$			Adults $\Sigma w_i = 0.94$		
		AIC_c (ΔAIC_c)	w_i	Rank	AIC_c (ΔAIC_c)	w_i	Rank	AIC_c (ΔAIC_c)	w_i	Rank
Human only	Effluent	99.59 (5.76)	0.013	12	79.40 (9.40)	0.004	12	105.62 (3.91)	0.042	6
	Sediment	98.94 (5.10)	0.018	9	79.52 (9.52)	0.003	14	106.94 (5.22)	0.022	8
	Fish catch	99.61 (5.78)	0.013	13	78.74 (8.74)	0.005	10	107.82 (6.11)	0.014	12
	Effluent, Sediment, Fish catch	103.93 (10.10)	0.002	17	83.94 (13.94)	0.000	17	110.01 (8.30)	0.005	17
Oceanography only	Wave power	99.46 (5.63)	0.014	11	79.51 (9.51)	0.004	13	107.27 (5.56)	0.018	11
	Sea surface temperature (SST)	99.8 (6.00)	0.012	15	78.78 (8.78)	0.005	11	106.99 (5.28)	0.021	9
	Chlorophyll- <i>a</i> (Chl- <i>a</i>)	95.97 (2.13)	0.081	5	77.67 (7.66)	0.009	8	103.94 (2.23)	0.098	4
	Wave power, SST, Chl- <i>a</i>	99.83 (6.00)	0.012	14	80.19 (10.19)	0.002	15	108.32 (6.61)	0.011	14
Habitat only	Depth mean	98.47 (4.64)	0.023	8	76.70 (6.70)	0.014	6	107.91 (6.20)	0.013	13
	Depth range	94.09 (0.26)	0.206	2	71.02 (1.02)	0.245	2	103.19 (1.47)	0.142	3
	Coral cover	95.11 (1.27)	0.124	4	70.00 (0.00)	0.408	1	104.55 (2.84)	0.072	5
	Rugosity	99.14 (5.30)	0.017	10	77.90 (7.90)	0.008	9	107.00 (5.29)	0.021	10

	Depth mean, Depth range, Coral cover, Rugosity	98.31 (4.47)	0.025	7	74.80 (4.80)	0.037	5	109.32 (7.61)	0.007	15
Mixed (Human, Habitat, Oceanography)	Effluent, Coral cover, Chl- <i>a</i>	94.54 (0.71)	0.164	3	72.59 (2.58)	0.112	4	101.71 (0.00)	0.298	1
	Sediment, Rugosity, Wave power	102.79 (8.96)	0.003	16	82.49 (12.49)	0.001	16	109.58 (7.86)	0.006	16
Mixed (Human, Habitat)	Fish catch, Depth range, Coral cover	93.84 (0.00)	0.234	1	72.30 (2.30)	0.129	3	102.85 (1.14)	0.168	2
Mixed (Human, Oceanography)	Effluent, Fish catch, Wave power	104.45 (10.61)	0.001	18	83.97 (13.97)	0.000	18	110.56 (8.85)	0.004	18
Null	--	97.47 (3.63)	0.038	6	77.12 (7.12)	0.012	7	105.85 (4.14)	0.038	7
Global	Effluent, Sediment, Fish catch, Wave power, SST, Chl- <i>a</i> , Depth mean, Depth range, Coral cover, Rugosity	104.92 (11.09)	0.001	19	86.86 (16.86)	0.000	19	117.79 (16.08)	0.000	19

Across life stages, coral cover and depth range consistently emerged as key predictors of occupancy (Figure 2). Relative variable importance values, which are calculated by summing the Akaike weights of all models that include a given covariate and therefore indicate how consistently a predictor appears in well-supported models, showed that habitat features had the highest relative influence, particularly for juveniles, whereas the importance of human and oceanographic predictors increased for adults (Figure 2). Model-averaged β estimates indicated weak individual effects, as the 95%, 80%, and 50% confidence intervals for all variables overlapped zero (Figure 3; Appendix Tables 12-14).

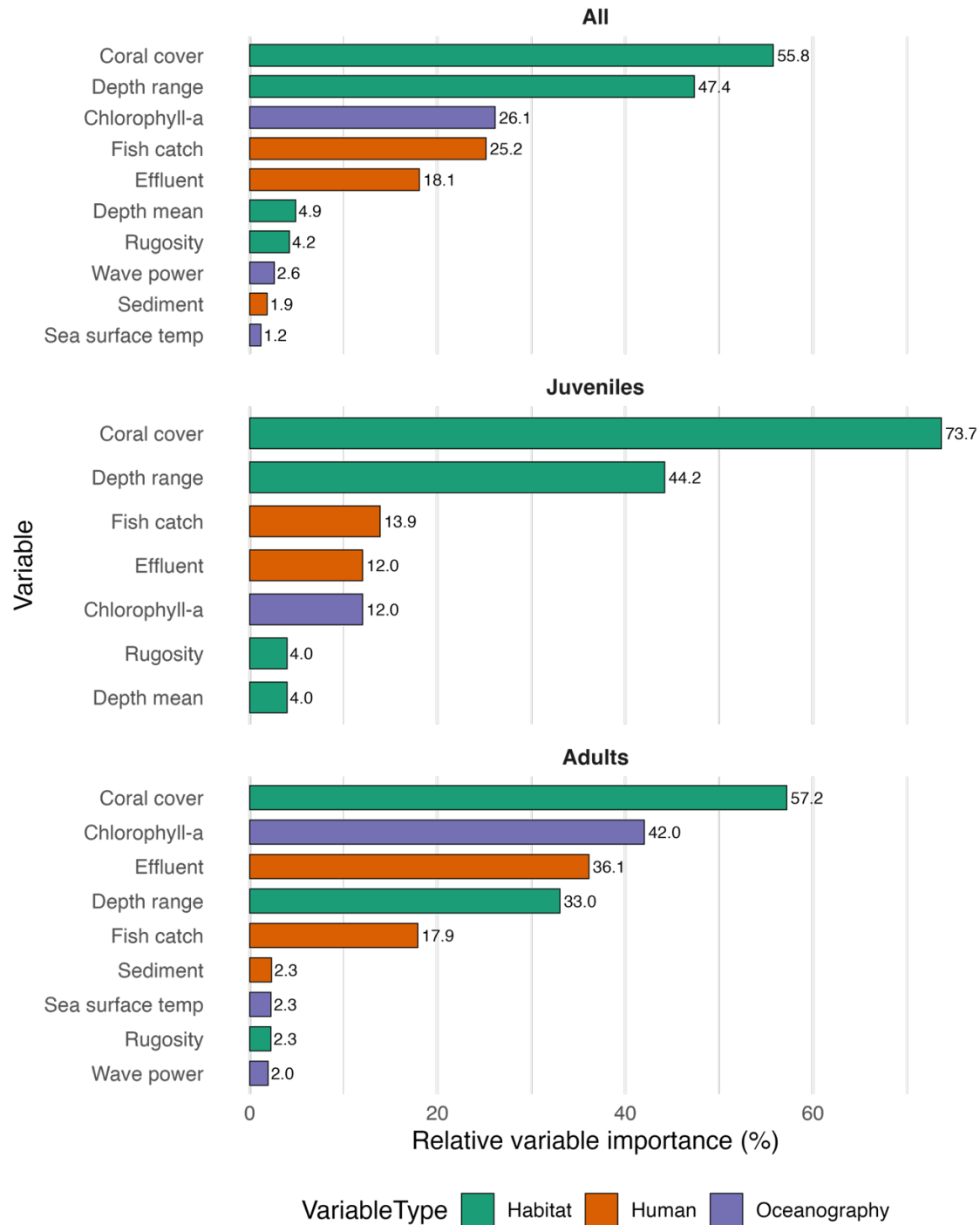


Figure 2. Relative variable importance for predictor variables across occupancy models for three life stages: All individuals, Juveniles, and Adults. Bars represent the relative importance of each variable, calculated as the summed Akaike weights of all models (in the confidence set, $\Delta AIC_c < 6$) containing that variable and rescaled following Cade (2015). Variables are color-coded by type (Habitat, Human, or Oceanography).

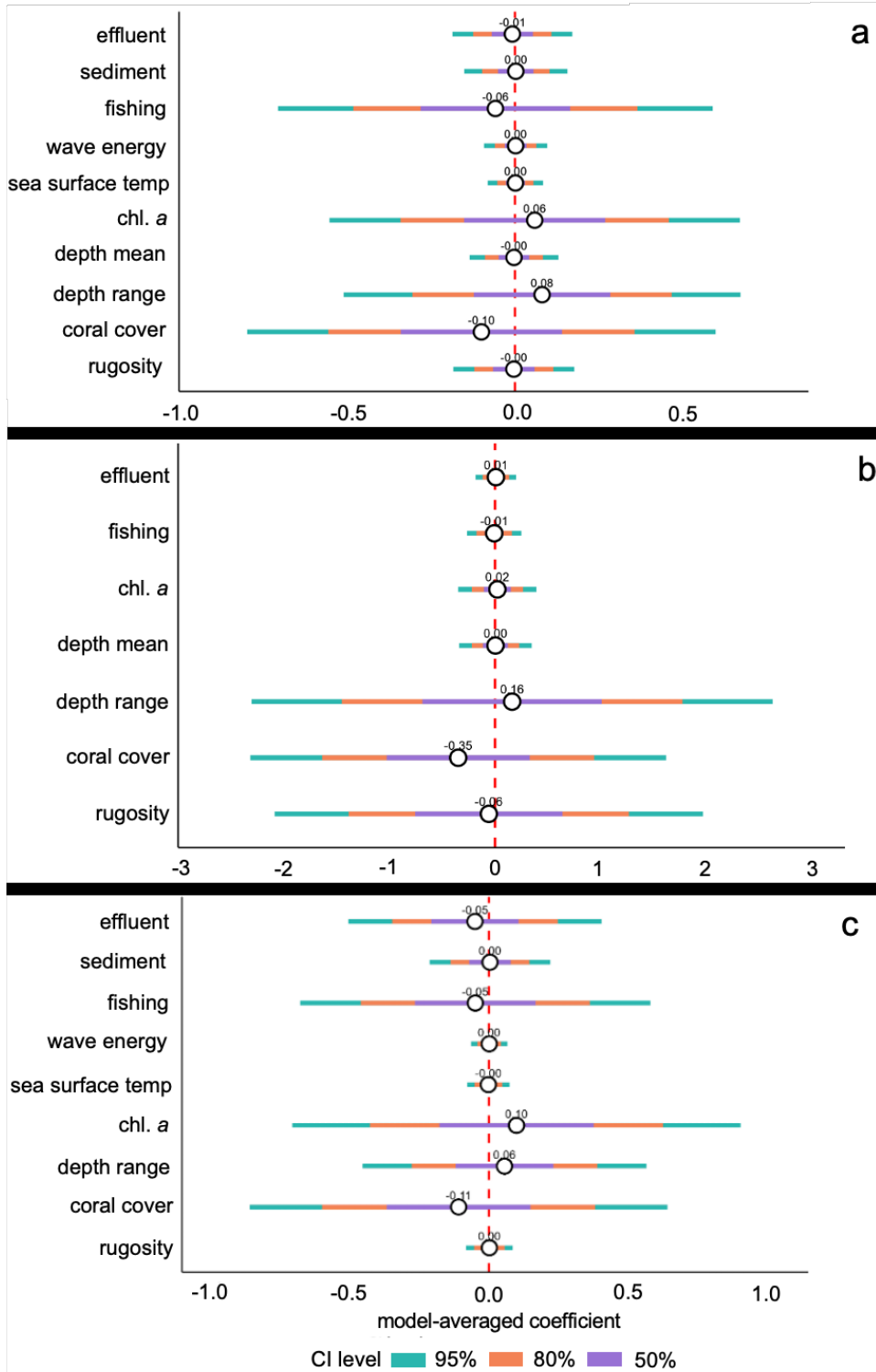


Figure 3. Model-averaged coefficient estimates (\pm 95% CI) for a.) "All", b.) "Juvenile", c.) "Adult" pāku'iku'i occupancy (ψ) across predictors in the confidence sets (models with $\Delta AIC_c < 6$). The red vertical line indicates no effect.

3.2 Two-Species Detection-Occupancy Model Results

The four *a priori* candidate models assessing the influence of adult pāku‘iku‘i presence on juvenile detection and occupancy and vice versa showed moderate model uncertainty with 2 models with $\Delta AIC_c < 2$ (Table 3). The top-ranked two-species occupancy model, which allowed juvenile and adult occupancy probabilities to vary but constrained detection probabilities to be equal across life stages ($\psi_A, \psi_{BA}, \psi_{Ba}, p_A = p_B = r_A = r_{BA} = r_{Ba}$), received the most support ($w_i = 0.53$), followed closely by a model that allowed occupancy to vary while permitting partial variation in detection ($\psi_A, \psi_{BA}, \psi_{Ba}, p_A = p_B, r_A, r_{BA} = r_{Ba}$) ($\Delta AIC_c = 0.49, w_i = 0.42$). The fully parameterized model that allowed both occupancy and all detection probabilities to vary independently received little support ($\Delta AIC_c = 4.86, w_i = 0.05$), and the null model, which constrained occupancy and detection to be equal across life stages, was unsupported ($\Delta AIC_c > 10$).

Table 3. Four *a priori* candidate models used to estimate percent areas occupied and detectability of adult and juvenile pāku‘iku‘i on Hawai‘i Island, HI, USA, 2024. Reported: AIC_c , ΔAIC_c , Akaike weight (w_i , calculated from ΔAIC_c), relative likelihood, number of parameters (K), and $-2 \log$ -likelihood (neg2ll).

Model	AIC_c	ΔAIC_c	w_i	Likelihood	K	neg2ll
psiA, psiBA, psiBa, pA = pB = rA = rBA = rBa	201.74	0.00	0.53	1.00	4	192.89
psiA, psiBA, psiBa, pA = pB, rA, rBA = rBa	202.24	0.49	0.42	0.78	5	190.93
psiA, psiBA, psiBa, pA, pB, rA, rBA, rBa	206.60	4.86	0.05	0.09	8	187.25
psiA = psiBA = psiBa, pA = pB = rA = rBA = rBa	219.20	17.45	0.00	0.00	2	214.95

AIC = Akaike’s Information Criterion, AIC_c = Akaike’s Information Criterion for small sample sizes, ΔAIC_c = differences in AIC_c , w_i = Akaike weights, Likelihood = relative likelihood of each model compared to the best model, K = number of parameters. psiA = probability that the area is occupied by juveniles, regardless of occupancy status of adults, psiBA = probability that the area is occupied by adults, given juveniles are present, psiBa = probability that the area is occupied by adults, given juveniles are not present, pA = probability of detecting juveniles, given adults are not present, pB = probability of detecting adults, given juveniles are not present, rA = probability of detecting juveniles, given both life stages are present, rBA = probability of detecting adults, given both life stages are present, and juveniles were detected, rBa = probability of detecting adults, given both life stages are present, and juveniles were not detected.

To account for model uncertainty, model-averaged estimates of occupancy and detection probabilities were derived from the full set of *a priori* models following Burnham and Anderson (2002, 2004; Appendix Table 7). Model-averaged estimates indicated moderate juvenile occupancy overall (Figure 4; $\psi_A = 0.23$, SE = 0.06, 95% CI = 0.11 – 0.35). Adult occupancy was strongly conditional on juvenile presence: the probability of adult occurrence when juveniles

were present was very high (Figure 4; $\psi_{BA} = 0.92$, SE = 0.12, 95% CI = 0.68 – 1.00), whereas adult occupancy when juveniles were absent was low (Figure 4; $\psi_{Ba} = 0.10$, SE = 0.05, 95% CI = 0.00 – 0.21), indicating a positive association between life stages. Detection probabilities were broadly similar across life stages and conditional states, with overlapping confidence intervals, but slightly lower estimate and widest confidence intervals for adult detection when both life stages were present but juveniles not detected (Appendix Table 7, Appendix Figure 3).

3.3 Detection Probability by Survey Method and Substrate

Detection probabilities differed between diver and ROV surveys, although these differences varied by life stage (Figure 4; Appendix Table 15). For all pāku‘iku‘i life stages combined, detection was slightly higher for divers ($p = 0.87$, SE = 0.08, 95% CI = 0.62, 0.97) than for ROV surveys ($p = 0.65$, SE = 0.14, 95% CI = 0.36, 0.86), though confidence intervals overlapped. Among adults, detection was similar between divers ($p = 0.62$, SE = 0.13, 95% CI = 0.36, 0.83) and ROVs ($p = 0.63$, SE = 0.20, 95% CI = 0.24, 0.90). In contrast, juvenile detection showed the greatest difference between methods: diver surveys yielded very high detection probability ($p = 0.91$, SE = 0.06, 95% CI = 0.70, 0.98), while ROV detection was substantially lower ($p = 0.32$, SE = 0.16, 95% CI = 0.10, 0.66).

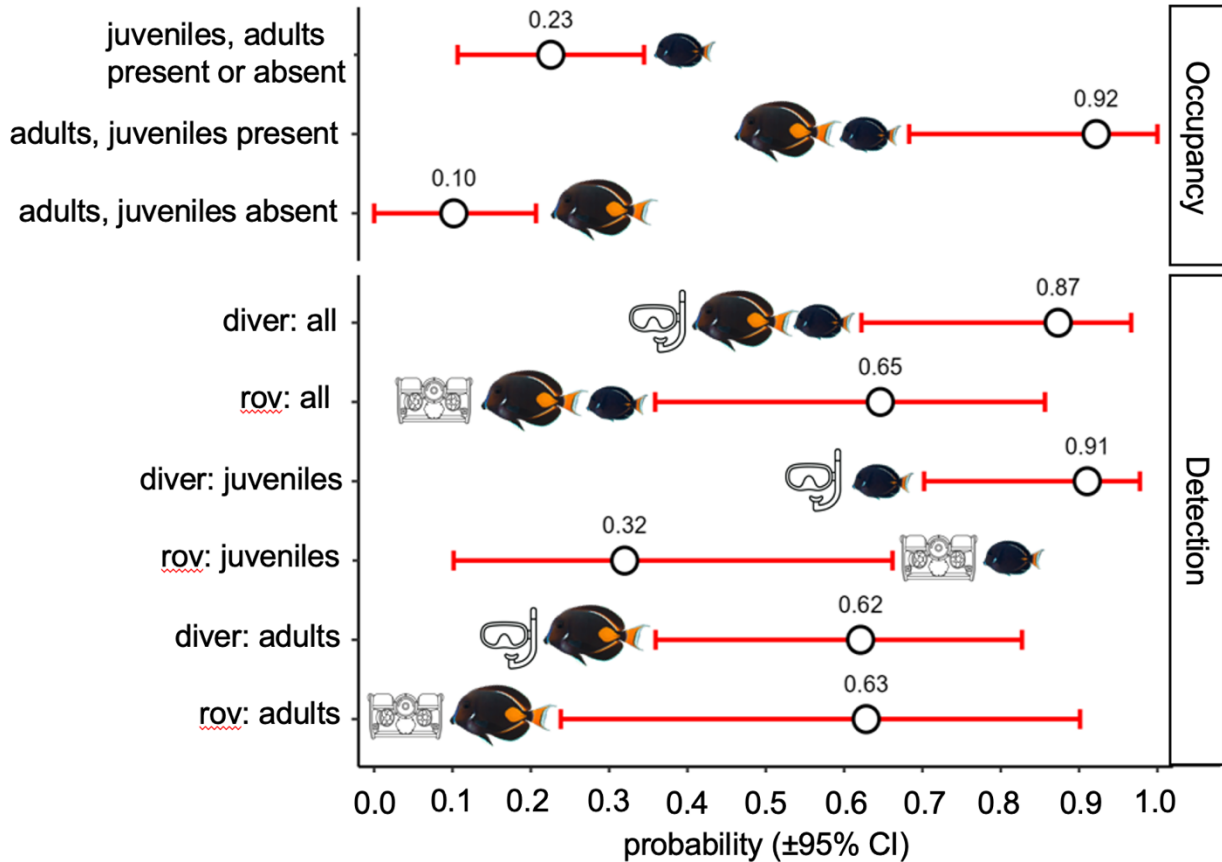


Figure 4. Combined occupancy and detection probabilities (\pm 95% CI) for pāku'iku'i across life stages and survey methods. Detection was modeled as a function of survey method (diver vs. ROV) across life stages (“All,” “Adults,” and “Juveniles”), with occupancy held constant.

Detection probability generally declined with increasing percent unconsolidated substrate across survey methods and life stages, although confidence intervals for the estimated slopes always overlapped zero, so only trends are described below (Appendix Table 16,17; Appendix Figure 4). For all pāku'iku'i life stages combined, unconsolidated substrate was negatively associated with detection probabilities of both diver-based surveys ($\beta = -5.02$, 95% CI = -13.69 , 3.66) and ROV-based surveys ($\beta = -13.50$, 95% CI = -36.70 , 9.69). Similarly negative trends were observed for adults (Diver: $\beta = -3.35$, 95% CI = -13.03 , 6.33; ROV: $\beta = -13.70$, 95% CI = -38.94 , 11.53) and juveniles (Diver: $\beta = -4.07$, 95% CI = -12.73 , 4.59; ROV: $\beta = -32.91$, 95% CI = -74.35 , 8.53).

3.4 Model Validation

External validation using the NOAA CREP dataset indicated that the model with all life stages exhibited statistically significant discriminatory ability between sites where pāku‘iku‘i were observed and those where they were absent (Appendix Table 18). Predicted detection–occupancy probabilities were generally low across sites, but median probabilities were slightly higher for sites where they were present (median = 0.48, interquartile range/IQR = 0.38–0.52, $n = 28$) compared to sites where they were absent (median = 0.40, IQR = 0.28–0.48, $n = 125$; Mann Whitney U-test $W = 1218.0$, $P = 0.01$; Appendix Table 19; Appendix Figure 5).

4. DISCUSSION

This study applied a multi-method occupancy modeling framework to examine how habitat, oceanographic, and anthropogenic factors influence the distribution and detectability of pāku‘iku‘i (*Acanthurus achilles*) around Hawai‘i Island. By accounting for imperfect detection and comparing life stages, we provide new insight into the ecological gradients shaping this culturally and ecologically important reef fish. Model averaging revealed depth range and coral cover appeared repeatedly in well-supported models, especially for juveniles, indicating that benthic complexity plays a central role in where pāku‘iku‘i occur. Oceanographic and human-use variables contributed more to adult distributions, though with weaker and more uncertain effects. Taken together, these model-averaged patterns suggest that pāku‘iku‘i occupancy reflects a blend of fine-scale habitat use and broader environmental context, while wide confidence intervals highlight the need to interpret individual effect sizes cautiously. While occupancy models had evidence of mild underdispersion, correction factors are typically only applied in

cases of overdispersion (Jones 2022), and the model diagnostic values (\hat{c}) indicated reasonable model fit. Thus, the underdispersion may reflect small sample size, limited variability in covariates across time, and low number of detections of this less common species.

These patterns also reflect broader challenges inherent to monitoring coral-reef fishes, where cryptic behavior (MacKenzie et al. 2006; Williams et al. 2006; MacNeil et al. 2010), complex habitat structure (Green et al. 2013; Suarez and Grabowski 2021), and variable survey conditions (Williams et al. 2006) can obscure true occupancy. The subtle and sometimes uncertain habitat signals detected here are consistent with the environments pāku‘iku‘i inhabit, including areas where visibility can be spatially inconsistent and fine-scale changes in depth, surge exposure, or coral structure can shift detectability from one survey to the next. The rarity of juveniles observed in pre-existing, long-term datasets, for example, may therefore stem as much from low detection as from ecological scarcity. By distinguishing true absence from non-detection, the occupancy framework clarifies when low encounter rates reflect biological patterns and when they reflect survey limitations (MacKenzie et al. 2002; Bachelor et al. 2014), an especially important distinction for species that transition across habitat types (Hoover 2008) and display life-stage-specific behaviors. In this way, the findings emphasize both the ecological complexity of pāku‘iku‘i life history and behavior, as well as the practical difficulty of reliably monitoring fishes in heterogeneous, dynamic reef environments.

4.1 Ontogenetic patterns of occupancy and life-stage connectivity

Coral cover and depth range were the strongest correlates of occupancy across all life stages, suggesting that benthic structure plays a central role in shaping spatial patterns of pāku‘iku‘i occurrence. Areas with variable coral cover and rapid changes in depth over short

distances create complex reef surfaces with ledges, crevices, and small openings that offer shelter from predators (Scharf et al. 2006). Juvenile fishes commonly rely on these types of microhabitats, and juvenile pāku‘iku‘i likely use deeper or more protected reef slopes for similar reasons, where structural relief softens surge and reduces predation risk during early growth (Scharf et al. 2006; Friedlander et al. 2003). These same features influence how herbivorous fishes use the habitat, since grazing activity and herbivore biomass are often concentrated in structurally complex, coral-dominated areas (Vergés et al. 2011). Depth-structured habitats may also function as a behavioral transition zone, allowing juveniles to remain in deeper, sheltered areas while they are still small, less aggressive, and vulnerable to predators, and then gradually move into shallower habitats as they mature (Scharf et al. 2006). As individuals increase in size and competitive ability, interactions with territorial adults in the shallows can facilitate this upward movement into higher-energy reef zones, where subadults eventually establish their own territories. In these shallow zones, territorial schools develop, which may reflect a feeding strategy to overcome other territorial fishes (L. Kaupu, *pers. comm.*). These processes may explain why our results found that more complex and steeply sloped habitats support higher probabilities of pāku‘iku‘i occupancy across life stages.

This ontogenetic pattern in habitat use aligns with broader spatial trends documented at larger scales. Our findings align with those of Layko and Donovan (2024), who identified structural habitat features, such as rugosity and depth, to be the most consistent predictors of pāku‘iku‘i presence across the main Hawaiian Islands. We also found the influence of human and oceanographic factors varied ontogenetically, with stronger effects on adults than on juveniles. This pattern is consistent with long-standing observations that adult pāku‘iku‘i occupy high-energy, shallow coastal environments, whereas juveniles are more often associated with

deeper, more protected reef slopes (Randall 2007; Hoover 2008). In support of this pattern, chlorophyll-*a* had the second highest variable importance among adult models, indicating that broad-scale patterns of ocean productivity may help structure adult distributions, with shallow fore-reef habitats likely providing higher algal growth and more frequent grazing opportunities for herbivorous fishes than deeper, slope reefs.

The two-species occupancy model revealed strong co-occurrence between juvenile and adult pāku‘iku‘i, with adults more likely to occur at sites where juveniles were present. This pattern, consistent with detection model results and anecdotal reports from former aquarium collectors (T. Grabowski, *pers. comm.*), suggests possible ecological dependencies such as conspecific settlement cues or protection by adults. Observations from the Miloli‘i Community-Based Subsistence Fishing Area indicate that adults “guide” juveniles into shallower waters (L. Kaupu *pers. comm.*), further reinforcing the potential for life stage overlap and social facilitation. These relationships may help explain the scarcity of juveniles in recent surveys showing adult population decline, underscoring the importance of demographic connectivity in reef fish monitoring and management.

Patterns in other herbivorous reef fishes show similar spatial overlap across depth gradients, where surgeonfishes and parrotfishes use continuous reef mosaics that extend from shallow to mid-depth habitats rather than being strictly segregated by age or size (Russ 2003; Adam et al. 2011). Studies have shown that herbivore biomass is typically highest in shallow fore-reef areas but remains substantial on deeper slopes when topographic relief is high (Nemeth and Appeldoorn 2009), indicating that structural complexity supports herbivore presence across a broad depth range. Russ (2003) further demonstrated that herbivorous fishes often concentrate where algal turf productivity is greatest rather than occupying fixed depth zones, suggesting that

food availability rather than depth alone shapes their spatial patterns. Research on parrotfishes in Moorea adds to this perspective by showing strong ontogenetic connectivity across habitats, with juveniles settling in lagoon nurseries and adults later moving onto the fore-reef (Adam et al. 2011). Together, these studies highlight that habitat structure, resource production, and cross-habitat linkages can create substantial life-stage overlap, providing a broader ecological context for the co-occurrence between juvenile and adult pāku‘iku‘i observed in this study.

4.2 Detection and methodological implications

Accounting for imperfect detection was critical to distinguish true ecological absence from non-detection. Detection probabilities (0.55 - 0.67) were broadly similar across life stages, indicating that detectability was not strongly influenced by age or co-occurrence. The lack of substantial variation across conditional states suggests that both juveniles and adults were equally likely to be recorded when present, regardless of survey method (diver vs. ROV). The pattern of slightly lower detection estimates coupled by wide confidence intervals for adults when juveniles were present but undetected likely reflects limited sample size rather than behavioral avoidance (Mckann et al. 2013; Lindfield et al. 2014; Gray et al. 2016). Overall, these results indicate moderate and consistent detectability, reinforcing that co-occurrence patterns reflect true occupancy dynamics rather than detection bias.

Comparing detection between survey methods highlights common challenges and trade-offs in coral-reef fish monitoring. Juveniles are often underrepresented because they occupy distinct habitats, are smaller, or exhibit more cryptic coloration (Ackerman & Bellwood 2000; Willis 2001; Gilbert et al. 2005; MacKenzie et al. 2006; Green et al. 2013). Modeling detection of juveniles revealed that divers had higher detection rates than ROVs, but ROVs provide

broader coverage and time/cost efficiency than divers (Sward et al. 2019), particularly in areas unsafe or impractical for divers. ROVs may also reduce observer bias and support consistent, noninvasive surveys across sites (Nalmpanti et al. 2022), though they have lower resolution than the human eye, which can limit their ability to distinguish small or cryptic individuals (Andaloro et al. 2013). Detection probability also declined with increasing unconsolidated substrate, reflecting both ecological and observational realities. Pāku‘iku‘i, like many reef fishes, rarely occupy sandy habitats where shelter and food resources are limited. Consistently negative relationships across diver and ROV methods indicate that substrate composition influences occupancy and detectability, underscoring the importance of structurally complex habitats in reef fish monitoring (Schultz et al. 2015). Nonetheless, ROVs could be a valuable complement to diver-based surveys in long-term, large-scale monitoring efforts as they could refine population assessments and allow for comparability among datasets using different techniques, which would be particularly valuable in tracking species recovery under fishery closures. Together, our results join the growing evidence that combining survey methods improves detection across habitats and life stages (Nichols et al. 2008; Gray et al. 2016; Green et al. 2013).

4.3 Management relevance, limitations, and future directions

Hawai‘i’s long-term monitoring programs have documented few juvenile pāku‘iku‘i despite extensive survey effort (DAR, *unpubl. data*). Our results suggest juveniles are present but less common and less detectable using standard monitoring surveys that are not specifically designed to detect patchily distributed early life stages. Adjusting how and where they are surveyed may improve detection. ROVs, while not a replacement for diver-based surveys, can complement them by expanding spatial coverage and enabling a greater number of surveys in

less time, particularly in deeper or surge-exposed habitats that are difficult to access safely with divers. At the survey rate observed during this study (≈ 10 transects in 3 hours), an ROV team could complete roughly 26 surveys in a standard 8-hour field day, allowing 3–4 times more site coverage than diver-based surveys at comparable effort. The expanded use of ROVs, however, must be balanced with logistical constraints such as high cost, operator training and expertise, and data processing requirements (Sward et al. 2019).

Although not used in this study, ROVs can be equipped with laser-scaling systems and programmed transects to systematically survey defined spatial areas at consistent heights above the seafloor. Integrating a small, pāku‘iku‘i-focused sampling module within existing surveys could complement standard diver transects by targeting habitats with high predicted occupancy, such as steep depth transitions and coral-rich slope breaks. Repeated visits to a subset of high-probability or previously occupied sites could improve juvenile detection, allow assessment of recruitment timing, and provide insight into persistence and life-stage transitions across years. Together, these adjustments could increase encounter rates and support more accurate evaluation of demographic connectivity while remaining compatible with existing monitoring frameworks.

Some of the environmental covariates used here represent past conditions rather than the current state of the reef, which limits our ability to interpret how ongoing impacts influence pāku‘iku‘i distributions. In particular, several Ocean Tipping Points variables (Wedding et al. 2018) are model-based estimates informed by assumptions about temporal and spatial processes, whereas the GAO habitat layers (Asner et al. 2020, 2022) are more recent, high-resolution empirical data collected directly from the reef environment, which may partly explain why GAO covariates showed stronger support in our models. While factors such as wave power may have changed little over time, land use and coastal development on Hawai‘i Island have expanded in

recent years, which could alter effluent inputs relative to older estimates, and fishing pressure may also have shifted during and after the aquarium fishery closure. Updated environmental and human-use datasets will be needed to determine whether these relationships reflect present conditions and to identify covariates with stronger explanatory power.

Looking ahead, this occupancy framework highlights how targeted sampling and multi-method surveys can reveal ecological patterns that are difficult to observe using single methods alone. By identifying where juveniles are most likely to occur and when they may be present, these results provide a clear path for refining survey design to improve detection across habitats and life stages. Integrating multi-method transects, surveying repeatedly during the recruitment season, and updating environmental datasets may allow managers to test hypotheses about demographic connectivity and early life-stage ecology while preserving the value of the long-term diver-based time series. The framework developed here for pāku‘iku‘i provides a model for other species and systems, strengthening the scientific foundation for reef conservation in Hawai‘i and beyond.

APPENDIX

Table 1. Habitat classification of combined depth, coral cover, and rugosity rasters into low, medium, and high categories using mean \pm 1 SD thresholds. Depth was classified as low (0-7.44 m), medium (7.45-14.178 m), and high (14.179-38.428 m). Coral cover was classified as low (0.001-7.7937%), medium (7.938-24.847%), and high (24.848-88%). Rugosity was classified as low (0-0.3294), medium (0.3295-0.6627), and high (0.6628-1). These classes were reclassified for raster summation and aggregated within a 25 \times 25 m fishnet for stratified random site selection. Colors correspond to those shown in survey maps.

Depth	Coral cover	Rugosity
Low	Low	Medium
Medium	Low	Medium
Low	Medium	Medium
Medium	Medium	Medium
Low	High	Medium
Medium	High	Medium
Low	Low	High
Medium	Low	High
High	Low	High
Low	Medium	High
Medium	Medium	High
High	Medium	High
Low	High	High
Medium	High	High
High	High	High

Table 2. Results of linear regressions used to estimate missing site values. Relationships are shown between in situ measurements and corresponding 25 m GIS covariates for depth and coral cover. Reported values include slope, intercept, coefficient of determination (R^2), adjusted R^2 , p-value, and sample size (n).

Response	Predictor	Slope	Intercept	R^2	Adjusted R^2	p-value	n
In-situ depth	GIS Depth	1.00	0.85	0.69	0.68	<0.01	48
In-situ coral	GIS Coral	1.06	8.99	0.39	0.38	<0.01	36

Table 3. Results of linear regressions used to estimate missing site values. Relationships are shown between in situ measurements and corresponding 100 m GIS covariates for depth and coral cover. Reported values include slope, intercept, coefficient of determination (R^2), adjusted R^2 , p-value, and sample size (n).

Response	Predictor	Slope	Intercept	R^2	Adjusted R^2	p-value	n
In-situ depth	GIS Depth	1.12	-0.65	0.66	0.66	<0.01	50
In-situ coral	GIS Coral	1.28	6.18	0.43	0.41	<0.01	42

Table 4. Cross-scale habitat model comparison for “All” dataset. Occupancy (ψ) was modeled using a candidate set of 80 models representing every possible combination of the four habitat covariates (coral cover, rugosity, mean depth, and depth range) measured at 25 m and 100 m spatial resolutions, with detection (p) held constant as method + percent unconsolidated substrate. Model labels encode covariate scale (e.g., coral_25, rugosity_25, depth_mean_100, depth_range_100) and are ranked by ΔAIC_c . Reported: Model number and parameterization, AIC_c , ΔAIC_c , Akaike weight (w_i , calculated from ΔAIC_c), number of parameters (k), and $-2 \log$ -likelihood (neg2ll).

Model # and Parameterization	AIC_c	ΔAIC_c	w_i	k	neg2ll
5)depth_range_100(ψ)method+unconsolidated(p)	94.09	0.00	0.06	5	82.79
31)depth_range_100+rugosity_25(ψ)method+unconsolidated(p)	94.74	0.65	0.06	6	80.88
21)depth_mean_100+depth_range_100(ψ)method+unconsolidated(p)	94.98	0.89	0.05	6	81.11
2)coral_25(ψ)method+unconsolidated(p)	95.11	1.01	0.04	5	83.80
16)coral_25+depth_range_100(ψ)method+unconsolidated(p)	95.23	1.13	0.04	6	81.36
55)depth_range_100+coral_25+rugosity_25(ψ)method+unconsolidated(p)	95.54	1.45	0.05	7	79.00
24)depth_mean_25+depth_range_100(ψ)method+unconsolidated(p)	95.54	1.45	0.04	6	81.68
29)depth_range_100+rugosity_100(ψ)method+unconsolidated(p)	95.73	1.63	0.03	6	81.86
13)coral_100+depth_range_100(ψ)method+unconsolidated(p)	95.74	1.64	0.03	6	81.87
53)depth_range_100+coral_100+rugosity_25(ψ)method+unconsolidated(p)	96.63	2.54	0.03	7	80.09
45)depth_mean_100+depth_range_100+rugosity_25(ψ)method+unconsolidated(p)	96.63	2.54	0.03	7	80.09
51)depth_range_100+coral_25+rugosity_100(ψ)method+unconsolidated(p)	96.64	2.54	0.03	7	80.09
46)depth_mean_25+depth_range_100+rugosity_25(ψ)method+unconsolidated(p)	97.08	2.99	0.02	7	80.54

37)depth_mean_100+depth_range_100+coral_25(ψ)method+unconsolidated(p)	97.15	3.05	0.02	7	80.60
41)depth_mean_100+depth_range_100+rugosity_100(ψ)method+unconsolidated(p)	97.21	3.12	0.02	7	80.67
49)depth_range_100+coral_100+rugosity_100(ψ)method+unconsolidated(p)	97.32	3.23	0.02	7	80.78
12)coral_25+depth_mean_100(ψ)method+unconsolidated(p)	97.48	3.38	0.01	6	83.61
38)depth_mean_25+depth_range_100+coral_25(ψ)method+unconsolidated(p)	97.56	3.47	0.02	7	81.01
20)coral_25+rugosity_100(ψ)method+unconsolidated(p)	97.56	3.47	0.01	6	83.69
10)coral_25+depth_mean_25(ψ)method+unconsolidated(p)	97.59	3.50	0.01	6	83.73
33)depth_mean_100+depth_range_100+coral_100(ψ)method+unconsolidated(p)	97.61	3.52	0.02	7	81.06
42)depth_mean_25+depth_range_100+rugosity_100(ψ)method+unconsolidated(p)	97.66	3.57	0.02	7	81.12
14)coral_25+depth_range_25(ψ)method+unconsolidated(p)	97.67	3.57	0.01	6	83.80
18)coral_25+rugosity_25(ψ)method+unconsolidated(p)	97.67	3.57	0.01	6	83.80
34)depth_mean_25+depth_range_100+coral_100(ψ)method+unconsolidated(p)	98.02	3.93	0.02	7	81.48
78)coral_25+depth_mean_25+depth_range_100+rugosity_25(ψ)method+unconsolidated(p)	98.30	4.20	0.02	8	78.95
74)coral_25+depth_mean_100+depth_range_100+rugosity_25(ψ)method+unconsolidated(p)	98.31	4.21	0.02	8	78.96
1)coral_100(ψ)method+unconsolidated(p)	98.33	4.24	0.01	5	87.03
3)depth_mean_100(ψ)method+unconsolidated(p)	98.47	4.38	0.01	5	87.17
7)rugosity_100(ψ)method+unconsolidated(p)	98.50	4.40	0.01	5	87.19

4)depth_mean_25(ψ)method+unconsolidated(p)	98.58	4.49	0.01	5	87.28
25)depth_mean_100+rugosity_100(ψ)method+unconsolidated(p)	98.87	4.78	0.01	6	85.01
8)rugosity_25(ψ)method+unconsolidated(p)	99.14	5.05	0.00	5	87.84
73)coral_25+depth_mean_100+depth_range_100+rugosity_100(ψ)method+unconsolidated(p)	99.21	5.12	0.01	8	79.87
66)coral_100+depth_mean_100+depth_range_100+rugosity_25(ψ)method+unconsolidated(p)	99.23	5.14	0.01	8	79.88
28)depth_mean_25+rugosity_100(ψ)method+unconsolidated(p)	99.34	5.25	0.01	6	85.47
6)depth_range_25(ψ)method+unconsolidated(p)	99.37	5.27	0.00	5	88.06
77)coral_25+depth_mean_25+depth_range_100+rugosity_100(ψ)method+unconsolidated(p)	99.40	5.31	0.01	8	80.05
70)coral_100+depth_mean_25+depth_range_100+rugosity_25(ψ)method+unconsolidated(p)	99.42	5.32	0.01	8	80.07
27)depth_mean_100+rugosity_25(ψ)method+unconsolidated(p)	99.42	5.33	0.01	6	85.55
17)coral_100+rugosity_100(ψ)method+unconsolidated(p)	99.69	5.60	0.00	6	85.82
26)depth_mean_25+rugosity_25(ψ)method+unconsolidated(p)	99.73	5.64	0.00	6	85.86
59)depth_mean_100+coral_25+rugosity_100(ψ)method+unconsolidated(p)	99.80	5.71	0.01	7	83.26
65)coral_100+depth_mean_100+depth_range_100+rugosity_100(ψ)method+unconsolidated(p)	99.82	5.72	0.01	8	80.47
15)coral_100+depth_range_25(ψ)method+unconsolidated(p)	99.90	5.81	0.00	6	86.03
69)coral_100+depth_mean_25+depth_range_100+rugosity_100(ψ)method+unconsolidated(p)	100.02	5.93	0.01	8	80.67
60)depth_mean_25+coral_25+rugosity_100(ψ)method+unconsolidated(p)	100.05	5.96	0.01	7	83.51

19)coral_100+rugosity_25(ψ)method+unconsolidated(p)	100.07	5.97	0.00	6	86.20
63)depth_mean_100+coral_25+rugosity_25(ψ)method+unconsolidated(p)	100.07	5.98	0.01	7	83.53
39)depth_mean_100+depth_range_25+coral_25(ψ)method+unconsolidated(p)	100.13	6.04	0.01	7	83.59
52)depth_range_25+coral_25+rugosity_100(ψ)method+unconsolidated(p)	100.23	6.13	0.01	7	83.68
64)depth_mean_25+coral_25+rugosity_25(ψ)method+unconsolidated(p)	100.24	6.15	0.01	7	83.70
40)depth_mean_25+depth_range_25+coral_25(ψ)method+unconsolidated(p)	100.26	6.17	0.01	7	83.72
23)depth_mean_100+depth_range_25(ψ)method+unconsolidated(p)	100.27	6.18	0.00	6	86.41
56)depth_range_25+coral_25+rugosity_25(ψ)method+unconsolidated(p)	100.34	6.25	0.00	7	83.80
22)depth_mean_25+depth_range_25(ψ)method+unconsolidated(p)	100.54	6.45	0.00	6	86.67
9)coral_100+depth_mean_100(ψ)method+unconsolidated(p)	100.64	6.55	0.00	6	86.77
11)coral_100+depth_mean_25(ψ)method+unconsolidated(p)	100.66	6.57	0.00	6	86.80
32)depth_range_25+rugosity_100(ψ)method+unconsolidated(p)	101.03	6.93	0.00	6	87.16
57)depth_mean_100+coral_100+rugosity_100(ψ)method+unconsolidated(p)	101.52	7.43	0.00	7	84.97
43)depth_mean_100+depth_range_25+rugosity_100(ψ)method+unconsolidated(p)	101.55	7.45	0.00	7	85.00
30)depth_range_25+rugosity_25(ψ)method+unconsolidated(p)	101.64	7.55	0.00	6	87.78
58)depth_mean_25+coral_100+rugosity_100(ψ)method+unconsolidated(p)	101.85	7.76	0.00	7	85.31
61)depth_mean_100+coral_100+rugosity_25(ψ)method+unconsolidated(p)	101.99	7.89	0.00	7	85.44

44)depth_mean_25+depth_range_25+rugosity_100(ψ)method+unconsolidated(p)	102.02	7.92	0.00	7	85.47
47)depth_mean_100+depth_range_25+rugosity_25(ψ)method+unconsolidated(p)	102.10	8.00	0.00	7	85.55
62)depth_mean_25+coral_100+rugosity_25(ψ)method+unconsolidated(p)	102.16	8.07	0.00	7	85.62
50)depth_range_25+coral_100+rugosity_100(ψ)method+unconsolidated(p)	102.17	8.07	0.00	7	85.62
35)depth_mean_100+depth_range_25+coral_100(ψ)method+unconsolidated(p)	102.33	8.24	0.00	7	85.79
48)depth_mean_25+depth_range_25+rugosity_25(ψ)method+unconsolidated(p)	102.41	8.31	0.00	7	85.86
36)depth_mean_25+depth_range_25+coral_100(ψ)method+unconsolidated(p)	102.43	8.33	0.00	7	85.88
54)depth_range_25+coral_100+rugosity_25(ψ)method+unconsolidated(p)	102.49	8.40	0.00	7	85.95
75)coral_25+depth_mean_100+depth_range_25+rugosity_100(ψ)method+unconsolidated(p)	102.59	8.50	0.00	8	83.24
79)coral_25+depth_mean_25+depth_range_25+rugosity_100(ψ)method+unconsolidated(p)	102.84	8.75	0.00	8	83.49
76)coral_25+depth_mean_100+depth_range_25+rugosity_25(ψ)method+unconsolidated(p)	102.88	8.78	0.00	8	83.53
80)coral_25+depth_mean_25+depth_range_25+rugosity_25(ψ)method+unconsolidated(p)	103.05	8.95	0.00	8	83.70
67)coral_100+depth_mean_100+depth_range_25+rugosity_100(ψ)method+unconsolidated(p)	104.30	10.20	0.00	8	84.95
71)coral_100+depth_mean_25+depth_range_25+rugosity_100(ψ)method+unconsolidated(p)	104.61	10.51	0.00	8	85.26
68)coral_100+depth_mean_100+depth_range_25+rugosity_25(ψ)method+unconsolidated(p)	104.76	10.67	0.00	8	85.41
72)coral_100+depth_mean_25+depth_range_25+rugosity_25(ψ)method+unconsolidated(p)	104.93	10.84	0.00	8	85.58

Table 5. Cross-scale habitat model comparison for “Juveniles” dataset. Occupancy (ψ) was modeled using a candidate set of 80 models representing every possible combination of the four habitat covariates (coral cover, rugosity, mean depth, and depth range) measured at 25 m and 100 m spatial resolutions, with detection (p) held constant as method + percent unconsolidated substrate. Model labels encode covariate scale (e.g., coral_25, rugosity_25, depth_mean_100, depth_range_100). Reported: Model number, Model parameters, Rank ΔAIC_c , AIC_c , ΔAIC_c , Akaike weight (w_i , calculated from ΔAIC_c), number of parameters (k), and $-2 \log$ -likelihood (neg2ll).

Model # and Parameterization	AIC_c	ΔAIC_c	w_i	k	neg2ll
66)coral_100+depth_mean_100+depth_range_100+rugosity_25(ψ)method+unconsolidated(p)	62.94	0	0.72	8	43.59
70)coral_100+depth_mean_25+depth_range_100+rugosity_25(ψ)method+unconsolidated(p)	68.1	5.16	0.05	8	48.75
33)depth_mean_100+depth_range_100+coral_100(ψ)method+unconsolidated(p)	69.13	6.19	0.02	7	52.58
34)depth_mean_25+depth_range_100+coral_100(ψ)method+unconsolidated(p)	69.13	6.19	0.02	7	52.58
24)depth_mean_25+depth_range_100(ψ)method+unconsolidated(p)	69.15	6.2	0.02	6	55.28
21)depth_mean_100+depth_range_100(ψ)method+unconsolidated(p)	69.62	6.67	0.01	6	55.75
16)coral_25+depth_range_100(ψ)method+unconsolidated(p)	69.77	6.83	0.01	6	55.9
2)coral_25(ψ)method+unconsolidated(p)	70	7.06	0.01	5	58.7
31)depth_range_100+rugosity_25(ψ)method+unconsolidated(p)	70.4	7.46	0.01	6	56.53
46)depth_mean_25+depth_range_100+rugosity_25(ψ)method+unconsolidated(p)	70.59	7.65	0.01	7	54.05
45)depth_mean_100+depth_range_100+rugosity_25(ψ)method+unconsolidated(p)	70.88	7.94	0.01	7	54.33
38)depth_mean_25+depth_range_100+coral_25(ψ)method+unconsolidated(p)	71	8.06	0.01	7	54.45
5)depth_range_100(ψ)method+unconsolidated(p)	71.02	8.08	0	5	59.71
37)depth_mean_100+depth_range_100+coral_25(ψ)method+unconsolidated(p)	71.2	8.25	0.01	7	54.65

42)depth_mean_25+depth_range_100+rugosity_100(ψ)method+unconsolidated(p)	71.72	8.78	0.01	7	55.18
51)depth_range_100+coral_25+rugosity_100(ψ)method+unconsolidated(p)	71.88	8.94	0.01	7	55.33
20)coral_25+rugosity_100(ψ)method+unconsolidated(p)	72.01	9.07	0	6	58.15
55)depth_range_100+coral_25+rugosity_25(ψ)method+unconsolidated(p)	72.08	9.14	0.01	7	55.54
10)coral_25+depth_mean_25(ψ)method+unconsolidated(p)	72.14	9.2	0	6	58.28
41)depth_mean_100+depth_range_100+rugosity_100(ψ)method+unconsolidated(p)	72.18	9.24	0	7	55.63
12)coral_25+depth_mean_100(ψ)method+unconsolidated(p)	72.38	9.44	0	6	58.51
13)coral_100+depth_range_100(ψ)method+unconsolidated(p)	72.49	9.54	0	6	58.62
14)coral_25+depth_range_25(ψ)method+unconsolidated(p)	72.55	9.61	0	6	58.69
18)coral_25+rugosity_25(ψ)method+unconsolidated(p)	72.56	9.62	0	6	58.7
28)depth_mean_25+rugosity_100(ψ)method+unconsolidated(p)	72.91	9.97	0	6	59.04
29)depth_range_100+rugosity_100(ψ)method+unconsolidated(p)	73.19	10.25	0	6	59.32
65)coral_100+depth_mean_100+depth_range_100+rugosity_100(ψ)method+unconsolidated(p)	73.39	10.45	0	8	54.04
60)depth_mean_25+coral_25+rugosity_100(ψ)method+unconsolidated(p)	73.52	10.58	0	7	56.97
77)coral_25+depth_mean_25+depth_range_100+rugosity_100(ψ)method+unconsolidated(p)	73.61	10.66	0	8	54.26
25)depth_mean_100+rugosity_100(ψ)method+unconsolidated(p)	73.7	10.76	0	6	59.84
78)coral_25+depth_mean_25+depth_range_100+rugosity_25(ψ)method+unconsolidated(p)	73.71	10.77	0	8	54.36
73)coral_25+depth_mean_100+depth_range_100+rugosity_100(ψ)method+unconsolidated(p)	73.78	10.84	0	8	54.44
59)depth_mean_100+coral_25+rugosity_100(ψ)method+unconsolidated(p)	73.82	10.88	0	7	57.28
22)depth_mean_25+depth_range_25(ψ)method+unconsolidated(p)	74.37	11.43	0	6	60.5

26)depth_mean_25+rugosity_25(ψ)method+unconsolidated(p)	74.49	11.55	0	6	60.62
64)depth_mean_25+coral_25+rugosity_25(ψ)method+unconsolidated(p)	74.6	11.66	0	7	58.06
52)depth_range_25+coral_25+rugosity_100(ψ)method+unconsolidated(p)	74.64	11.7	0	7	58.09
49)depth_range_100+coral_100+rugosity_100(ψ)method+unconsolidated(p)	74.64	11.7	0	7	58.09
40)depth_mean_25+depth_range_25+coral_25(ψ)method+unconsolidated(p)	74.66	11.72	0	7	58.12
58)depth_mean_25+coral_100+rugosity_100(ψ)method+unconsolidated(p)	74.77	11.82	0	7	58.22
74)coral_25+depth_mean_100+depth_range_100+rugosity_25(ψ)method+unconsolidated(p)	74.8	11.86	0	8	55.45
63)depth_mean_100+coral_25+rugosity_25(ψ)method+unconsolidated(p)	74.94	12	0	7	58.39
39)depth_mean_100+depth_range_25+coral_25(ψ)method+unconsolidated(p)	74.96	12.01	0	7	58.41
56)depth_range_25+coral_25+rugosity_25(ψ)method+unconsolidated(p)	75.23	12.29	0	7	58.68
4)depth_mean_25(ψ)method+unconsolidated(p)	75.29	12.35	0	5	63.98
44)depth_mean_25+depth_range_25+rugosity_100(ψ)method+unconsolidated(p)	75.57	12.63	0	7	59.03
7)rugosity_100(ψ)method+unconsolidated(p)	75.63	12.69	0	5	64.32
27)depth_mean_100+rugosity_25(ψ)method+unconsolidated(p)	75.71	12.77	0	6	61.84
23)depth_mean_100+depth_range_25(ψ)method+unconsolidated(p)	75.78	12.83	0	6	61.91
57)depth_mean_100+coral_100+rugosity_100(ψ)method+unconsolidated(p)	75.79	12.85	0	7	59.25
53)depth_range_100+coral_100+rugosity_25(ψ)method+unconsolidated(p)	75.94	12.99	0	7	59.39
79)coral_25+depth_mean_25+depth_range_25+rugosity_100(ψ)method+unconsolidated(p)	76.32	13.37	0	8	56.97
43)depth_mean_100+depth_range_25+rugosity_100(ψ)method+u	76.35	13.41	0	7	59.81

nconsolidated(p)					
75)coral_25+depth_mean_100+depth_range_25+rugosity_100(ψ)method+unconsolidated(p)	76.62	13.68	0	8	57.27
69)coral_100+depth_mean_25+depth_range_100+rugosity_100(ψ)method+unconsolidated(p)	76.66	13.72	0	8	57.31
3)depth_mean_100(ψ)method+unconsolidated(p)	76.7	13.75	0	5	65.39
17)coral_100+rugosity_100(ψ)method+unconsolidated(p)	76.94	13.99	0	6	63.07
62)depth_mean_25+coral_100+rugosity_25(ψ)method+unconsolidated(p)	76.98	14.04	0	7	60.43
36)depth_mean_25+depth_range_25+coral_100(ψ)method+unconsolidated(p)	77.02	14.08	0	7	60.47
48)depth_mean_25+depth_range_25+rugosity_25(ψ)method+unconsolidated(p)	77.04	14.1	0	7	60.49
80)coral_25+depth_mean_25+depth_range_25+rugosity_25(ψ)method+unconsolidated(p)	77.18	14.23	0	8	57.83
71)coral_100+depth_mean_25+depth_range_25+rugosity_100(ψ)method+unconsolidated(p)	77.43	14.49	0	8	58.09
11)coral_100+depth_mean_25(ψ)method+unconsolidated(p)	77.78	14.84	0	6	63.92
76)coral_25+depth_mean_100+depth_range_25+rugosity_25(ψ)method+unconsolidated(p)	77.83	14.89	0	8	58.49
8)rugosity_25(ψ)method+unconsolidated(p)	77.9	14.96	0	5	66.59
15)coral_100+depth_range_25(ψ)method+unconsolidated(p)	78.02	15.08	0	6	64.16
1)coral_100(ψ)method+unconsolidated(p)	78.05	15.11	0	5	66.75
32)depth_range_25+rugosity_100(ψ)method+unconsolidated(p)	78.19	15.24	0	6	64.32
35)depth_mean_100+depth_range_25+coral_100(ψ)method+unconsolidated(p)	78.28	15.34	0	7	61.73
61)depth_mean_100+coral_100+rugosity_25(ψ)method+unconsolidated(p)	78.29	15.35	0	7	61.75
47)depth_mean_100+depth_range_25+rugosity_25(ψ)method+unconsolidated(p)	78.31	15.37	0	7	61.76
6)depth_range_25(ψ)method+unconsolidated(p)	78.34	15.4	0	5	67.04

67)coral_100+depth_mean_100+depth_range_25+rugosity_100(ψ)method+unconsolidated(p)	78.57	15.62	0	8	59.22
19)coral_100+rugosity_25(ψ)method+unconsolidated(p)	78.61	15.67	0	6	64.74
9)coral_100+depth_mean_100(ψ)method+unconsolidated(p)	79.25	16.3	0	6	65.38
50)depth_range_25+coral_100+rugosity_100(ψ)method+unconsolidated(p)	79.46	16.52	0	7	62.91
72)coral_100+depth_mean_25+depth_range_25+rugosity_25(ψ)method+unconsolidated(p)	79.79	16.85	0	8	60.44
30)depth_range_25+rugosity_25(ψ)method+unconsolidated(p)	80.35	17.41	0	6	66.48
54)depth_range_25+coral_100+rugosity_25(ψ)method+unconsolidated(p)	80.49	17.55	0	7	63.95
68)coral_100+depth_mean_100+depth_range_25+rugosity_25(ψ)method+unconsolidated(p)	81.06	18.12	0	8	61.72

Table 6. Cross-scale habitat model comparison for “Adults” dataset. Occupancy (ψ) was modeled using a candidate set of 80 models representing every possible combination of the four habitat covariates (coral cover, rugosity, mean depth, and depth range) measured at 25 m and 100 m spatial resolutions, with detection (p) held constant as method + percent unconsolidated substrate. Model labels encode covariate scale (e.g., coral_25, rugosity_25, depth_mean_100, depth_range_100) and are ranked by ΔAIC_c . Reported: Model number and parameterization, AIC_c , ΔAIC_c , Akaike weight (w_i , calculated from ΔAIC_c), number of parameters (k), and $-2 \log$ -likelihood (neg2ll).

Model # and Parameterization	AIC_c	ΔAIC_c	w_i	k	neg2ll
5)depth_range_100(ψ)method+unconsolidated(p)	103.19	0	0.09	5	91.88
2)coral_25(ψ)method+unconsolidated(p)	104.55	1.37	0.04	5	93.25
16)coral_25+depth_range_100(ψ)method+unconsolidated(p)	104.78	1.59	0.05	6	90.91
31)depth_range_100+rugosity_25(ψ)method+unconsolidated(p)	105.02	1.83	0.05	6	91.15
21)depth_mean_100+depth_range_100(ψ)method+unconsolidated(p)	105.31	2.12	0.04	6	91.44
29)depth_range_100+rugosity_100(ψ)method+unconsolidated(p)	105.35	2.16	0.04	6	91.48
24)depth_mean_25+depth_range_100(ψ)method+unconsolidated(p)	105.52	2.34	0.04	6	91.66
13)coral_100+depth_range_100(ψ)method+unconsolidated(p)	105.65	2.47	0.03	6	91.78
7)rugosity_100(ψ)method+unconsolidated(p)	106.52	3.33	0.02	5	95.22
55)depth_range_100+coral_25+rugosity_25(ψ)method+unconsolidated(p)	106.57	3.38	0.03	7	90.02
20)coral_25+rugosity_100(ψ)method+unconsolidated(p)	106.76	3.58	0.02	6	92.9
51)depth_range_100+coral_25+rugosity_100(ψ)method+unconsolidated(p)	106.88	3.7	0.03	7	90.34
14)coral_25+depth_range_25(ψ)method+unconsolidated(p)	106.89	3.71	0.02	6	93.03
18)coral_25+rugosity_25(ψ)method+unconsolidated(p)	106.93	3.74	0.02	6	93.06
8)rugosity_25(ψ)method+unconsolidated(p)	107	3.81	0.01	5	95.69
10)coral_25+depth_mean_25(ψ)method+unconsolidated(p)	107.06	3.87	0.02	6	93.19
12)coral_25+depth_mean_100(ψ)method+unconsolidated(p)	107.1	3.92	0.02	6	93.24

6)depth_range_25(ψ)method+unconsolidated(p)	107.25	4.07	0.01	5	95.95
37)depth_mean_100+depth_range_100+coral_25(ψ)method+unconsolidated(p)	107.39	4.2	0.02	7	90.84
38)depth_mean_25+depth_range_100+coral_25(ψ)method+unconsolidated(p)	107.46	4.27	0.02	7	90.91
45)depth_mean_100+depth_range_100+rugosity_25(ψ)method+unconsolidated(p)	107.56	4.38	0.02	7	91.02
53)depth_range_100+coral_100+rugosity_25(ψ)method+unconsolidated(p)	107.64	4.46	0.02	7	91.1
46)depth_mean_25+depth_range_100+rugosity_25(ψ)method+unconsolidated(p)	107.68	4.49	0.02	7	91.13
41)depth_mean_100+depth_range_100+rugosity_100(ψ)method+unconsolidated(p)	107.76	4.58	0.02	7	91.22
1)coral_100(ψ)method+unconsolidated(p)	107.87	4.68	0.01	5	96.56
3)depth_mean_100(ψ)method+unconsolidated(p)	107.91	4.73	0.01	5	96.61
49)depth_range_100+coral_100+rugosity_100(ψ)method+unconsolidated(p)	107.91	4.73	0.02	7	91.37
42)depth_mean_25+depth_range_100+rugosity_100(ψ)method+unconsolidated(p)	107.92	4.73	0.02	7	91.37
4)depth_mean_25(ψ)method+unconsolidated(p)	107.93	4.74	0.01	5	96.62
33)depth_mean_100+depth_range_100+coral_100(ψ)method+unconsolidated(p)	107.97	4.79	0.01	7	91.43
34)depth_mean_25+depth_range_100+coral_100(ψ)method+unconsolidated(p)	108.2	5.02	0.01	7	91.66
25)depth_mean_100+rugosity_100(ψ)method+unconsolidated(p)	108.3	5.11	0.01	6	94.43
28)depth_mean_25+rugosity_100(ψ)method+unconsolidated(p)	108.52	5.33	0.01	6	94.65
27)depth_mean_100+rugosity_25(ψ)method+unconsolidated(p)	108.6	5.41	0.01	6	94.73
26)depth_mean_25+rugosity_25(ψ)method+unconsolidated(p)	108.75	5.56	0.01	6	94.88
17)coral_100+rugosity_100(ψ)method+unconsolidated(p)	108.78	5.6	0.01	6	94.92
15)coral_100+depth_range_25(ψ)method+unconsolidated(p)	108.89	5.7	0.01	6	95.02

32)depth_range_25+rugosity_100(ψ)method+unconsolidated(p)	108.97	5.79	0.01	6	95.11
78)coral_25+depth_mean_25+depth_range_100+rugosity_25(ψ)method+unconsolidated(p)	109.05	5.86	0.01	8	89.7
19)coral_100+rugosity_25(ψ)method+unconsolidated(p)	109.11	5.92	0.01	6	95.24
23)depth_mean_100+depth_range_25(ψ)method+unconsolidated(p)	109.17	5.98	0.01	6	95.3
74)coral_25+depth_mean_100+depth_range_100+rugosity_25(ψ)method+unconsolidated(p)	109.32	6.13	0.01	8	89.97
22)depth_mean_25+depth_range_25(ψ)method+unconsolidated(p)	109.34	6.15	0.01	6	95.47
59)depth_mean_100+coral_25+rugosity_100(ψ)method+unconsolidated(p)	109.41	6.23	0.01	7	92.87
52)depth_range_25+coral_25+rugosity_100(ψ)method+unconsolidated(p)	109.41	6.23	0.01	7	92.87
30)depth_range_25+rugosity_25(ψ)method+unconsolidated(p)	109.43	6.24	0.01	6	95.56
60)depth_mean_25+coral_25+rugosity_100(ψ)method+unconsolidated(p)	109.44	6.26	0.01	7	92.9
56)depth_range_25+coral_25+rugosity_25(ψ)method+unconsolidated(p)	109.55	6.36	0.01	7	93
40)depth_mean_25+depth_range_25+coral_25(ψ)method+unconsolidated(p)	109.55	6.37	0.01	7	93.01
39)depth_mean_100+depth_range_25+coral_25(ψ)method+unconsolidated(p)	109.57	6.39	0.01	7	93.03
63)depth_mean_100+coral_25+rugosity_25(ψ)method+unconsolidated(p)	109.59	6.4	0.01	7	93.04
64)depth_mean_25+coral_25+rugosity_25(ψ)method+unconsolidated(p)	109.61	6.42	0.01	7	93.06
77)coral_25+depth_mean_25+depth_range_100+rugosity_100(ψ)method+unconsolidated(p)	109.61	6.42	0.01	8	90.26
73)coral_25+depth_mean_100+depth_range_100+rugosity_100(ψ)method+unconsolidated(p)	109.69	6.5	0.01	8	90.34
11)coral_100+depth_mean_25(ψ)method+unconsolidated(p)	110.36	7.18	0	6	96.5
9)coral_100+depth_mean_100(ψ)method+unconsolidated(p)	110.37	7.18	0	6	96.5

66)coral_100+depth_mean_100+depth_range_100+rugosity_25(ψ)method+unconsolidated(p)	110.37	7.18	0.01	8	91.02
70)coral_100+depth_mean_25+depth_range_100+rugosity_25(ψ)method+unconsolidated(p)	110.45	7.26	0.01	8	91.1
65)coral_100+depth_mean_100+depth_range_100+rugosity_100(ψ)method+unconsolidated(p)	110.57	7.38	0.01	8	91.22
69)coral_100+depth_mean_25+depth_range_100+rugosity_100(ψ)method+unconsolidated(p)	110.69	7.5	0.01	8	91.34
43)depth_mean_100+depth_range_25+rugosity_100(ψ)method+unconsolidated(p)	110.88	7.7	0	7	94.34
57)depth_mean_100+coral_100+rugosity_100(ψ)method+unconsolidated(p)	110.96	7.78	0	7	94.42
44)depth_mean_25+depth_range_25+rugosity_100(ψ)method+unconsolidated(p)	111.12	7.93	0	7	94.57
50)depth_range_25+coral_100+rugosity_100(ψ)method+unconsolidated(p)	111.19	8	0	7	94.64
58)depth_mean_25+coral_100+rugosity_100(ψ)method+unconsolidated(p)	111.19	8.01	0	7	94.65
47)depth_mean_100+depth_range_25+rugosity_25(ψ)method+unconsolidated(p)	111.21	8.02	0	7	94.66
61)depth_mean_100+coral_100+rugosity_25(ψ)method+unconsolidated(p)	111.28	8.09	0	7	94.73
48)depth_mean_25+depth_range_25+rugosity_25(ψ)method+unconsolidated(p)	111.38	8.2	0	7	94.84
62)depth_mean_25+coral_100+rugosity_25(ψ)method+unconsolidated(p)	111.41	8.23	0	7	94.87
54)depth_range_25+coral_100+rugosity_25(ψ)method+unconsolidated(p)	111.45	8.26	0	7	94.9
35)depth_mean_100+depth_range_25+coral_100(ψ)method+unconsolidated(p)	111.51	8.33	0	7	94.97
36)depth_mean_25+depth_range_25+coral_100(ψ)method+unconsolidated(p)	111.56	8.37	0	7	95.01
75)coral_25+depth_mean_100+depth_range_25+rugosity_100(ψ)method+unconsolidated(p)	112.19	9	0	8	92.84
79)coral_25+depth_mean_25+depth_range_25+rugosity_100(ψ)	112.22	9.03	0	8	92.87

method+unconsolidated(p)					
76)coral_25+depth_mean_100+depth_range_25+rugosity_25(ψ) method+unconsolidated(p)	112.34	9.15	0	8	92.99
80)coral_25+depth_mean_25+depth_range_25+rugosity_25(ψ)m ethod+unconsolidated(p)	112.35	9.16	0	8	93
67)coral_100+depth_mean_100+depth_range_25+rugosity_100(ψ)method+unconsolidated(p)	113.69	10.5	0	8	94.34
71)coral_100+depth_mean_25+depth_range_25+rugosity_100(ψ) method+unconsolidated(p)	113.87	10.68	0	8	94.52
68)coral_100+depth_mean_100+depth_range_25+rugosity_25(ψ) method+unconsolidated(p)	114	10.81	0	8	94.65
72)coral_100+depth_mean_25+depth_range_25+rugosity_25(ψ) method+unconsolidated(p)	114.12	10.93	0	8	94.77

Table 7. *A priori* detection-only model set used to evaluate covariates influencing detectability (p) of pāku'iku'i across life stages ("All," "Juveniles," and "Adults"). Occupancy (ψ) was held constant while detection was modeled as a function of survey- and habitat-level covariates. Reported: AIC_c , ΔAIC_c , Akaike weight (w_i , calculated from ΔAIC_c), relative likelihood, number of parameters (k), and $-2 \log$ -likelihood (neg2ll).

Life Stage	Model Parameterization	AIC_c	ΔAIC_c	w_i	Likelihood	K	neg2ll
All	1(ψ)method+unconsolidated(p)	97.47	0.00	0.95	1.00	4	88.62
	1(ψ)method+live_coral+dead_coral+unconsolidated+hard(p)	103.48	6.01	0.05	0.12	7	86.93
	1(ψ)method+depth+live_coral(p)	118.07	20.60	0.00	0.00	5	106.76
	1(ψ)method+depth(p)	119.49	22.02	0.00	0.00	4	110.64
	1(ψ)method+duration(p)	119.70	22.24	0.00	0.00	4	110.85
	1(ψ)method(p)	120.27	22.80	0.00	0.00	3	113.77
	1(ψ)1(p)	121.18	23.72	0.00	0.00	2	116.94
	1(ψ)method+dead_coral(p)	122.23	24.76	0.00	0.00	4	113.38
	1(ψ)method+live_coral(p)	122.28	24.81	0.00	0.00	4	113.43
	1(ψ)method+sum_substrates_pct(p)	122.28	24.81	0.00	0.00	4	113.43
	1(ψ)method+start_hour(p)	122.30	24.83	0.00	0.00	4	113.45
	1(ψ)method+hard(p)	122.31	24.85	0.00	0.00	4	113.46
Juveniles	1(ψ)method+unconsolidated(p)	77.12	0.00	0.85	1.00	4	68.27
	1(ψ)method+live_coral+dead_coral+unconsolidated+hard(p)	81.03	3.91	0.12	0.33	7	64.49
	1(ψ)method+depth+live_coral(p)	85.86	8.74	0.01	0.02	5	74.56
	1(ψ)method+depth(p)	86.36	9.25	0.01	0.01	4	77.51
	1(ψ)method+hard(p)	87.45	10.33	0.00	0.01	4	78.60
	1(ψ)method(p)	89.95	12.83	0.00	0.00	3	83.45
	1(ψ)method+live_coral(p)	91.20	14.08	0.00	0.00	4	82.35

	1(ψ)method+sum_substrates_pct(p)	91.20	14.08	0.00	0.00	4	82.35
	1(ψ)method+duration(p)	91.51	14.39	0.00	0.00	4	82.66
	1(ψ)method+dead_coral(p)	92.14	15.03	0.00	0.00	4	83.29
	1(ψ)method+start_hour(p)	92.30	15.19	0.00	0.00	4	83.45
	1(ψ)1(p)	98.30	21.19	0.00	0.00	2	94.06
Adults	1(ψ)method+unconsolidated(p)	105.85	0.00	0.90	1.00	4	97.00
	1(ψ)method+live_coral+dead_coral+unconsolidated+hard(p)	110.34	4.49	0.10	0.25	7	93.80
	1(ψ)method+depth(p)	119.64	13.79	0.00	0.00	4	110.79
	1(ψ)method+hard(p)	120.95	15.10	0.00	0.00	4	112.10
	1(ψ)method+depth+live_coral(p)	121.96	16.11	0.00	0.00	5	110.65
	1(ψ)1(p)	122.71	16.86	0.00	0.00	2	118.46
	1(ψ)method+dead_coral(p)	124.13	18.28	0.00	0.00	4	115.27
	1(ψ)method(p)	124.94	19.09	0.00	0.00	3	118.44
	1(ψ)method+live_coral(p)	125.22	19.37	0.00	0.00	4	116.37
	1(ψ)method+sum_substrates_pct(p)	125.22	19.37	0.00	0.00	4	116.37
	1(ψ)method+duration(p)	125.74	19.89	0.00	0.00	4	116.89
	1(ψ)method+start_hour(p)	126.46	20.61	0.00	0.00	4	117.61

Table 8. Model-averaged parameter estimates, standard errors, and 95% lower and upper confidence intervals for various occupancy and detection metrics from the single-season, two-species occupancy model for juvenile and adult pāku‘iku‘i on Hawai‘i Island, HI, USA, 2024.

Parameter	Estimate	SE	Lower 95% CI	Upper 95% CI
psiA	0.23	0.06	0.11	0.35
psiBA	0.92	0.12	0.68	1.00
psiBa	0.10	0.05	0.00	0.21
pA	0.66	0.10	0.47	0.86
pB	0.65	0.09	0.48	0.82
rA	0.67	0.06	0.55	0.79
rBA	0.55	0.17	0.23	0.88
rBa	0.67	0.06	0.55	0.78

psiA = probability that the area is occupied by juveniles, regardless of occupancy status of adults, psiBA = probability that the area is occupied by adults, given juveniles are present, psiBa = probability that the area is occupied by adults, given juveniles are not present, pA = probability of detecting juveniles, given adults are not present, pB = probability of detecting adults, given juveniles are not present, rA = probability of detecting juveniles, given both life stages are present, rBA = probability of detecting adults, given both life stages are present, and juveniles were detected, rBa = probability of detecting adults, given both life stages are present, and juveniles were not detected.

Table 9. Results of the single-season occupancy analysis for the “All” dataset, showing the models ranked by AIC_c from a set of 19 *a priori* candidates. Reported: model group (Human, Oceanography, Habitat, Mixed, Null, Global), model number and parameterization, AIC_c , ΔAIC_c , number of parameters (k), overdispersion estimate (\hat{c}), $-2 \log$ -likelihood (neg2ll), and Akaike weight (w_i , calculated from ΔAIC_c).

Model Group	Model # and Parameterization	AIC_c	ΔAIC_c	w_i	k	\hat{c}	neg2ll
Mixed (Human + Habitat)	16)fishing+depth_range+coral(ψ)method+unconsolidated(p)	93.84	0.00	0.23	7	0.84	77.29
Habitat	10)depth_range(ψ)method+unconsolidated(p)	94.09	0.26	0.21	5	0.84	82.79
Mixed (Human + Habitat + Ocean)	14)effluent+coral+chl(ψ)method+unconsolidated(p)	94.54	0.71	0.16	7	0.84	78.00
Habitat	11)coral(ψ)method+unconsolidated(p)	95.11	1.27	0.12	5	0.84	83.80
Ocean	7)chl(ψ)method+unconsolidated(p)	95.97	2.13	0.08	5	0.84	84.66
Null	18)1(ψ)method+unconsolidated(p)	97.47	3.63	0.04	4	0.84	88.62
Habitat	13)depth_mean+depth_range+coral+rugosity(ψ)method+unconsolidated(p)	98.31	4.47	0.03	8	0.84	78.96
Habitat	9)depth_mean(ψ)method+unconsolidated(p)	98.47	4.64	0.02	5	0.84	87.17
Human-Drivers	2)sediment(ψ)method+unconsolidated(p)	98.94	5.10	0.02	5	0.84	87.63
Habitat	12)rugosity(ψ)method+unconsolidated(p)	99.14	5.30	0.02	5	0.84	87.84
Ocean	5)wave(ψ)method+unconsolidated(p)	99.46	5.63	0.01	5	0.84	88.16
Human-Drivers	1)effluent(ψ)method+unconsolidated(p)	99.59	5.76	0.01	5	0.84	88.29
Human-Drivers	3)fishing(ψ)method+unconsolidated(p)	99.61	5.78	0.01	5	0.84	88.31
Ocean	8)wave+sst+chl(ψ)method+unconsolidated(p)	99.83	6.00	0.01	7	0.84	83.29
Physical	6)sst(ψ)method+unconsolidated(p)	99.84	6.00	0.01	5	0.84	88.54

Oceanography							
Mixed (Human + Habitat + Ocean)	15)sediment+rugosity+wave(ψ)method+unconsolidated(p)	102.79	8.96	0.00	7	0.84	86.25
Human-Drivers	4)effluent+sediment+fishing(ψ)method+unconsolidated(p)	103.93	10.10	0.00	7	0.84	87.39
Mixed (Human + Habitat + Ocean)	17)effluent+fishing+wave(ψ)method+unconsolidated(p)	104.45	10.61	0.00	7	0.84	87.90
Global	19)effluent+sediment+fishing+wave+sst+chl+depth_mean+depth_range+rugosity+coral(ψ)method+unconsolidated(p)	104.92	11.09	0.00	14	0.84	65.57

Table 10. Results of the single-season occupancy analysis for the “Juveniles” dataset, showing the models ranked by AIC_c from a set of 19 *a priori* candidates. Reported: model group (Human, Oceanography, Habitat, Mixed, Null, Global), model number and parameterization, AIC_c , ΔAIC_c , number of parameters (k), overdispersion estimate (\hat{c}), $-2 \log$ -likelihood (neg2ll), and Akaike weight (w_i , calculated from ΔAIC_c).

Model Group	Model # and Parameterization	AIC_c	ΔAIC_c	w_i	k	\hat{c}	neg2ll
Habitat	11)coral(ψ)method+unconsolidated(p)	70.00	0.00	0.41	5	0.45	58.70
Habitat	10)depth_range(ψ)method+unconsolidated(p)	71.02	1.02	0.25	5	0.45	59.71
Mixed (Human + Habitat)	16)fishing+depth_range+coral(ψ)method+unconsolidated(p)	72.30	2.30	0.13	7	0.45	55.75
Mixed (Human + Habitat + Ocean)	14)effluent+coral+chl(ψ)method+unconsolidated(p)	72.59	2.58	0.11	7	0.45	56.04
Habitat	13)depth_mean+depth_range+coral+rugosity(ψ)method+unconsolidated(p)	74.80	4.80	0.04	8	0.45	55.45
Habitat	9)depth_mean(ψ)method+unconsolidated(p)	76.70	6.70	0.01	5	0.45	65.39
Null	18)1(ψ)method+unconsolidated(p)	77.12	7.12	0.01	4	0.45	68.27
Ocean	7)chl(ψ)method+unconsolidated(p)	77.67	7.66	0.01	5	0.45	66.36
Habitat	12)rugosity(ψ)method+unconsolidated(p)	77.90	7.90	0.01	5	0.45	66.59
Human-Drivers	3)fishing(ψ)method+unconsolidated(p)	78.74	8.74	0.01	5	0.45	67.44
Ocean	6)sst(ψ)method+unconsolidated(p)	78.78	8.78	0.01	5	0.45	67.48
Human-Drivers	1)effluent(ψ)method+unconsolidated(p)	79.40	9.40	0.00	5	0.45	68.10
Ocean	5)wave(ψ)method+unconsolidated(p)	79.51	9.51	0.00	5	0.45	68.21
Human-Drivers	2)sediment(ψ)method+unconsolidated(p)	79.52	9.52	0.00	5	0.45	68.22

Ocean	8)wave+sst+chl(ψ)method+unconsolidated(p)	80.19	10.19	0.00	7	0.45	63.65
Mixed (Human + Habitat + Ocean)	15)sediment+rugosity+wave(ψ)method+unconsolidated(p)	82.49	12.49	0.00	7	0.45	65.95
Human-Drivers	4)effluent+sediment+fishing(ψ)method+unconsolidated(p)	83.94	13.94	0.00	7	0.45	67.40
Mixed (Human + Habitat + PhysOc)	17)effluent+fishing+wave(ψ)method+unconsolidated(p)	83.97	13.97	0.00	7	0.45	67.43
Global	19)effluent+sediment+fishing+wave+sst+chl+depth_mean+depth_range+rugosity+coral(ψ)method+unconsolidated(p)	86.86	16.86	0.00	14	0.45	47.51

Table 11. Results of the single-season occupancy analysis for the “Adults” dataset, showing the models ranked by AIC_c from a set of 19 *a priori* candidates. Reported: model group (Human, Oceanography, Habitat, Mixed, Null, Global), model number and parameterization, AIC_c , ΔAIC_c , number of parameters (k), overdispersion estimate (\hat{c}), $-2 \log$ -likelihood (neg2ll), and Akaike weight (w_i , calculated from ΔAIC_c).

Model Group	Model # and Parameterization	AIC_c	ΔAIC_c	w_i	k	\hat{c}	neg2ll
Mixed (Human + Habitat + Ocean)	14)effluent+coral+chl(ψ)method+unconsolidated(p)	101.71	0.00	0.30	7	0.83	85.17
Mixed (Human + Habitat)	16)fishing+depth_range+coral(ψ)method+unconsolidated(p)	102.85	1.14	0.17	7	0.83	86.31
Habitat	10)depth_range(ψ)method+unconsolidated(p)	103.19	1.47	0.14	5	0.83	91.88
Ocean	7)chl(ψ)method+unconsolidated(p)	103.94	2.23	0.10	5	0.83	92.64
Habitat	11)coral(ψ)method+unconsolidated(p)	104.55	2.84	0.07	5	0.83	93.25
Human-Drivers	1)effluent(ψ)method+unconsolidated(p)	105.62	3.91	0.04	5	0.83	94.32
Null	18)1(ψ)method+unconsolidated(p)	105.85	4.14	0.04	4	0.83	97.00
Human-Drivers	2)sediment(ψ)method+unconsolidated(p)	106.94	5.22	0.02	5	0.83	95.63
Ocean	6)sst(ψ)method+unconsolidated(p)	106.99	5.28	0.02	5	0.83	95.69
Habitat	12)rugosity(ψ)method+unconsolidated(p)	107.00	5.29	0.02	5	0.83	95.69
Physical Oceanography	5)wave(ψ)method+unconsolidated(p)	107.27	5.56	0.02	5	0.83	95.97
Human-Drivers	3)fishing(ψ)method+unconsolidated(p)	107.82	6.11	0.01	5	0.83	96.52
Habitat	9)depth_mean(ψ)method+unconsolidated(p)	107.91	6.20	0.01	5	0.83	96.61
Ocean	8)wave+sst+chl(ψ)method+unconsolidated(p)	108.32	6.61	0.01	7	0.83	91.78
Habitat	13)depth_mean+depth_range+cor	109.32	7.61	0.01	8	0.83	89.97

	al+rugosity(ψ)method+unconsolidated(p)						
Mixed (Human + Habitat + Ocean)	15)sediment+rugosity+wave(ψ)method+unconsolidated(p)	109.58	7.86	0.01	7	0.83	93.03
Human-Drivers	4)effluent+sediment+fishing(ψ)method+unconsolidated(p)	110.01	8.30	0.00	7	0.83	93.46
Mixed (Human + Habitat + Ocean)	17)effluent+fishing+wave(ψ)method+unconsolidated(p)	110.56	8.85	0.00	7	0.83	94.01
Global	19)effluent+sediment+fishing+wave+sst+chl+depth_mean+depth_range+rugosity+coral(ψ)method+unconsolidated(p)	117.79	16.08	0.00	14	0.83	78.44

Table 12. Model-averaged β coefficients (\pm SE) and confidence limits (95%, 80%, 50%) for detection (p) and occupancy (ψ) parameters from the “All” dataset, based on the subset of 19 candidate models with $\Delta AIC_c < 6$. Estimates were obtained using multimodel inference following Burnham and Anderson (2002) to account for model-selection uncertainty.

param	term	averaged beta	SE	LCL95	UCL95	LCL80	UCL80	LCL50	UCL50
p	p1_B1.Int	-1.39	3.12	-7.51	4.73	-5.39	2.61	-3.49	0.72
	p1_B1.Int. p.unconsolidated	-3.20	6.98	-16.88	10.48	-12.14	5.74	-7.91	1.51
	p2_B2	-0.18	0.48	-1.13	0.77	-0.80	0.44	-0.51	0.15
psi	psi_A1.Int	-0.01	0.20	-0.40	0.39	-0.27	0.25	-0.14	0.13
	psi_A1.Int. psi.effluent	-0.01	0.09	-0.19	0.17	-0.13	0.11	-0.07	0.05
	psi_A1.Int. psi.sediment	0.00	0.08	-0.15	0.16	-0.10	0.10	-0.05	0.06
	psi_A1.Int. psi.fishing	-0.06	0.33	-0.71	0.60	-0.49	0.37	-0.28	0.17
	psi_A1.Int. psi.wave	0.00	0.05	-0.09	0.10	-0.06	0.06	-0.03	0.03
	psi_A1.Int. psi.sst	0.00	0.04	-0.08	0.08	-0.05	0.06	-0.03	0.03
	psi_A1.Int. psi.chl	0.06	0.32	-0.56	0.68	-0.34	0.46	-0.15	0.27
	psi_A1.Int. psi.depth_mean	0.00	0.07	-0.14	0.13	-0.09	0.08	-0.05	0.04
	psi_A1.Int. psi.depth_range	0.08	0.30	-0.52	0.68	-0.31	0.47	-0.12	0.29
	psi_A1.Int. psi.coral	-0.10	0.36	-0.81	0.60	-0.56	0.36	-0.34	0.14
	psi_A1.Int. psi.rugosity	0.00	0.09	-0.19	0.18	-0.12	0.12	-0.07	0.06

Table 13. Model-averaged β coefficients (\pm SE) and confidence limits (95%, 80%, 50%) for detection (p) and occupancy (ψ) parameters from the “Juveniles” dataset, based on the subset of 19 candidate models with $\Delta AIC_c < 6$. Estimates were obtained using multimodel inference following Burnham and Anderson (2002) to account for model-selection uncertainty.

param	term	averaged beta	SE	LCL95	UCL95	LCL80	UCL80	LCL50	UCL50
p	p1_B1.Int	-1.39	3.33	-7.93	5.14	-5.67	2.88	-3.64	0.85
	p1_B1.Int.p.unconsolidated	-3.43	7.71	-18.55	11.69	-13.31	6.46	-8.63	1.77
	p2_B2	-0.48	1.04	-2.52	1.55	-1.81	0.85	-1.18	0.22
psi	psi_A1.Int	-0.21	0.57	-1.33	0.90	-0.94	0.52	-0.60	0.17
	psi_A1.Int.psi.effluent	0.01	0.10	-0.19	0.20	-0.12	0.13	-0.06	0.07
	psi_A1.Int.psi.fishing	-0.01	0.13	-0.27	0.25	-0.18	0.16	-0.10	0.08
	psi_A1.Int.psi.chlorophyll	0.02	0.19	-0.35	0.40	-0.22	0.27	-0.11	0.15
	psi_A1.Int.psi.depth_mean	0.00	0.18	-0.34	0.35	-0.22	0.23	-0.11	0.12
	psi_A1.Int.psi.depth_range	0.16	1.27	-2.32	2.64	-1.46	1.79	-0.69	1.02
	psi_A1.Int.psi.conductivity	-0.35	1.01	-2.33	1.63	-1.65	0.94	-1.03	0.33
	psi_A1.Int.psi.rugosity	-0.06	1.04	-2.10	1.98	-1.39	1.27	-0.76	0.64

Table 14. Model-averaged β coefficients (\pm SE) and confidence limits (95%, 80%, 50%) for detection (p) and occupancy (ψ) parameters from the “Adults” dataset, based on the subset of 19 candidate models with $\Delta AIC_c < 6$. Estimates were obtained using multimodel inference following Burnham and Anderson (2002) to account for model-selection uncertainty.

param	term	averaged beta	SE	LCL95	UCL95	LCL80	UCL80	LCL50	UCL50
p	p1_B1.Int	-1.38	3.06	-7.37	4.61	-5.30	2.54	-3.44	0.68
	p1_B1.Int.p .unconsolid ated	-2.70	5.94	-14.33	8.94	-10.31	4.91	-6.70	1.31
	p2_B2	0.03	0.28	-0.51	0.58	-0.32	0.39	-0.15	0.22
psi	psi_A1.Int	-0.04	0.23	-0.49	0.41	-0.33	0.25	-0.19	0.11
	psi_A1.Int. psi.effluent	-0.05	0.23	-0.51	0.41	-0.35	0.25	-0.21	0.11
	psi_A1.Int. psi.sedimen t	0.00	0.11	-0.21	0.22	-0.14	0.15	-0.07	0.08
	psi_A1.Int. psi.fishing	-0.05	0.32	-0.68	0.58	-0.46	0.36	-0.27	0.17
	psi_A1.Int. psi.wave	0.00	0.03	-0.06	0.07	-0.04	0.04	-0.02	0.02
	psi_A1.Int. psi.sst	0.00	0.04	-0.08	0.07	-0.05	0.05	-0.03	0.02
	psi_A1.Int. psi.chl	0.10	0.41	-0.71	0.91	-0.43	0.63	-0.18	0.38
	psi_A1.Int. psi.depth_ra nge	0.06	0.26	-0.45	0.57	-0.28	0.39	-0.12	0.23
	psi_A1.Int. psi.coral	-0.11	0.38	-0.86	0.64	-0.60	0.38	-0.37	0.15
	psi_A1.Int. psi.rugosity	0.00	0.04	-0.08	0.09	-0.05	0.06	-0.03	0.03

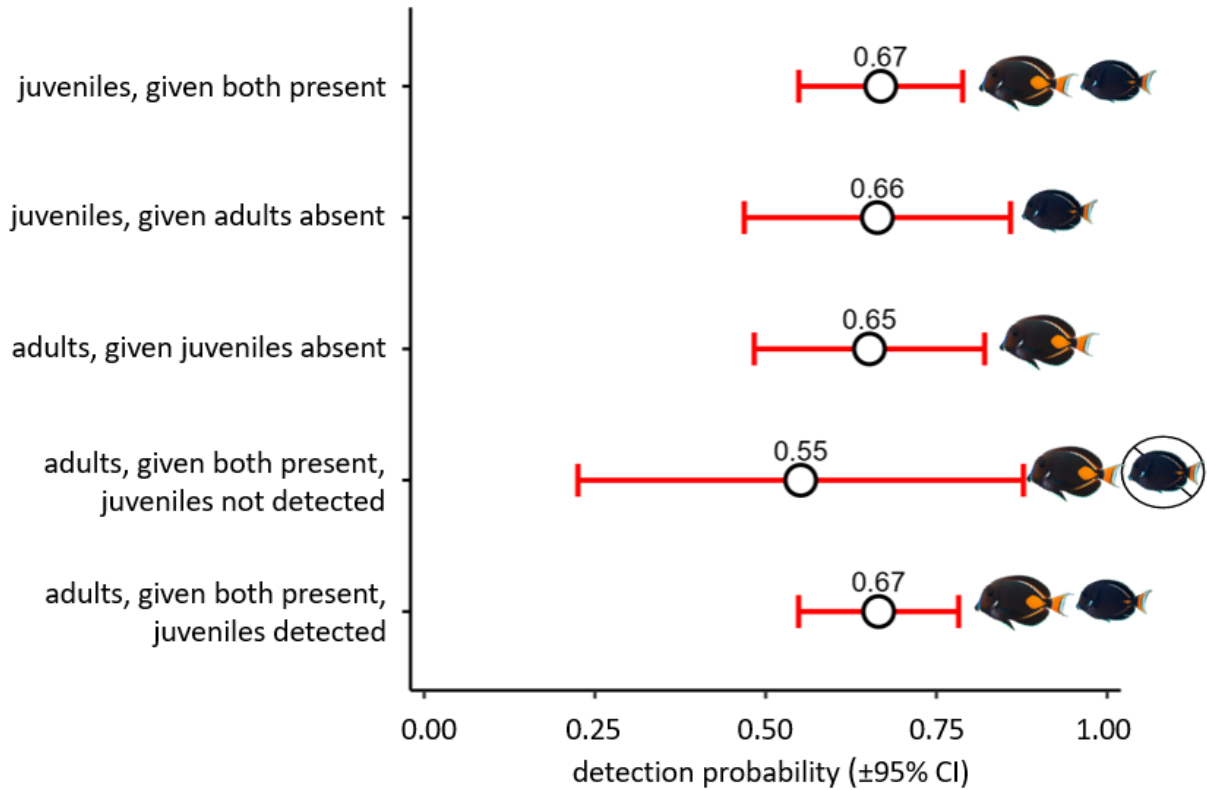


Figure 3. Detection probabilities ($\pm 95\%$ CI) for juvenile and adult pāku'iku'i under different conditional states. Detection probabilities were similar across life stages and conditions, with overlapping confidence intervals.

Table 15. Life stage, method, estimates, standard errors, 95% lower and upper confidence intervals, and lower and upper error bar lengths for detection rates from the single-season, single-species, multi-method detection model for all life stages, juvenile, and adult pāku'iku'i on Hawai'i Island, HI, USA, 2024.

Life Stage	Method	Estimate	SE	Lower 95% CI	Upper 95% CI	Lower error bar length	Upper error bar length
All	Diver	0.87	0.08	0.62	0.97	0.25	0.09
	ROV	0.65	0.14	0.36	0.86	0.29	0.21
Juveniles	Diver	0.91	0.06	0.70	0.98	0.21	0.07
	ROV	0.32	0.16	0.10	0.66	0.22	0.34
Adults	Diver	0.62	0.13	0.36	0.83	0.26	0.21
	ROV	0.63	0.20	0.24	0.90	0.39	0.27

Table 16. Coefficients from logistic regression models describing pāku‘iku‘i detection probability as a function of standardized percent unconsolidated substrate and survey method across life stages (“All,” “Juveniles,” and “Adults”). Each model includes an intercept and slope term for both diver and ROV methods. Estimates are presented on the logit scale, with corresponding lower and upper 95% confidence intervals. Intercepts represent the predicted log-odds of detection at the mean standardized unconsolidated substrate value ($z = 0$), and slopes (β) represent the change in log-odds of detection per one standard deviation increase in standardized unconsolidated substrate.

Life Stage	Method	Term	Estimate	Lower 95% CI	Upper 95% CI
All	Diver	Intercept	-2.57	-7.22	2.08
		Slope	-5.02	-13.69	3.66
Juveniles	ROV	Intercept	-8.11	-20.60	4.38
		Slope	-13.50	-36.70	9.69
	Diver	Intercept	-2.25	-6.90	2.40
		Slope	-4.07	-12.73	4.59
Adults	ROV	Intercept	-19.90	-42.95	3.14
		Slope	-32.91	-74.35	8.53
	Diver	Intercept	-2.55	-7.77	2.68
		Slope	-3.35	-13.03	6.33
	ROV	Intercept	-8.31	-21.97	5.35
		Slope	-13.70	-38.94	11.53

Table 17. Estimated slopes ($\beta \pm 95\%$ confidence intervals) from logistic regression models relating pāku‘iku‘i detection probability to standardized percent unconsolidated substrate across life stages and survey methods. Slopes (β) represent the change in logit-scale detection probability per one standard deviation increase in standardized unconsolidated substrate (z -score). Negative values indicate decreasing detection with increasing unconsolidated substrate. Diver was treated as the baseline method.

Life Stage	Method	Estimate	SE	Lower 95% CI	Upper 95% CI
All	Diver	-5.02	4.43	-13.69	3.66
	ROV	-13.50	5.94	-25.14	-1.87
Juveniles	Diver	-4.07	4.42	-12.73	4.59
	ROV	-32.91	16.13	-64.52	-1.30
Adults	Diver	-3.55	4.94	-13.03	6.33
	ROV	-13.70	6.21	-25.88	-1.53

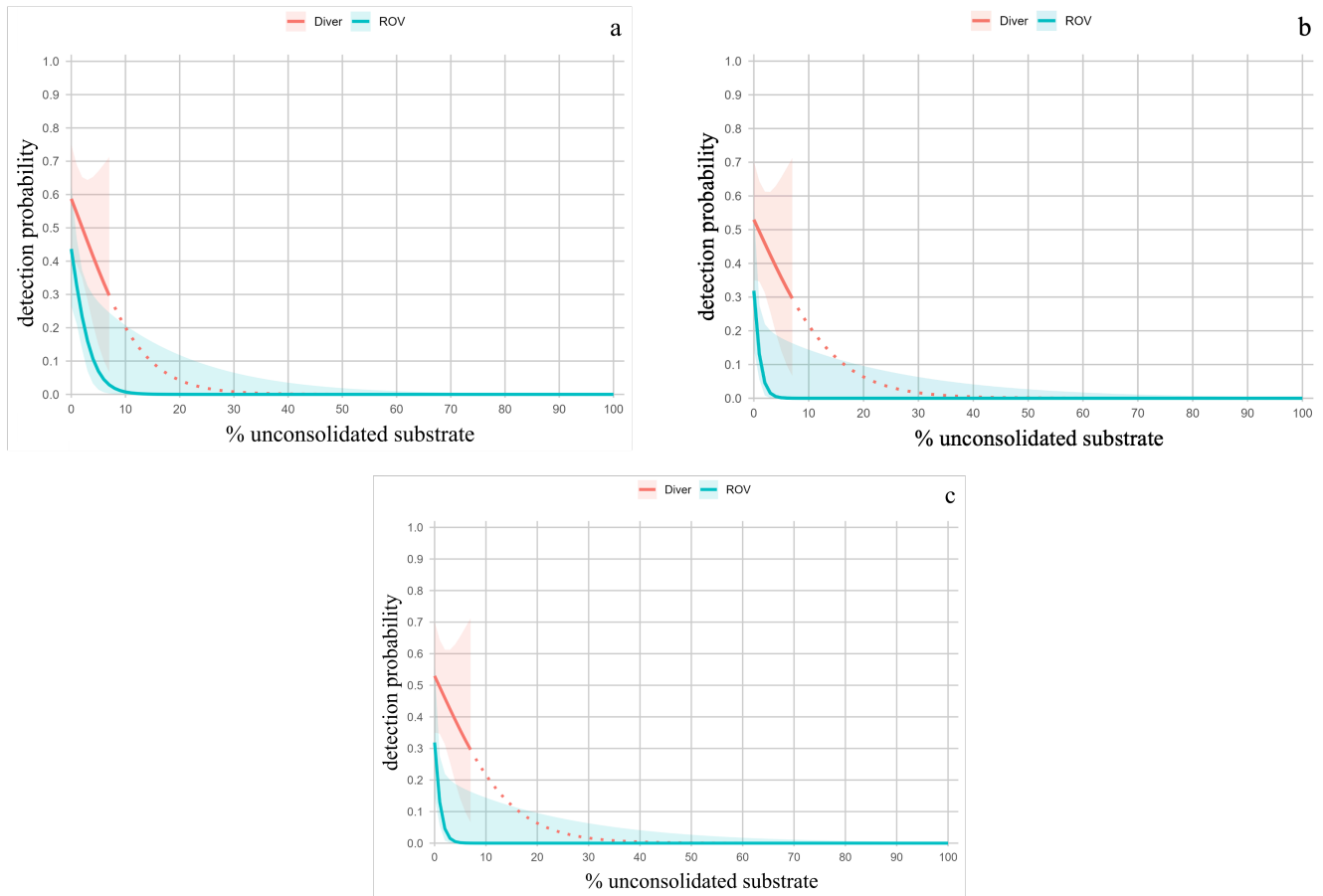


Figure 4. Predicted detection probability versus percent unconsolidated substrate for Diver and ROV surveys using the a.) “All”, b.) “Juvenile”, and c.) “Adult” datasets. Lines show model predictions from a single-season logistic regression with a method \times substrate interaction; shaded ribbons are 95% confidence intervals. The Diver line is solid across the observed substrate range and dotted where extrapolated beyond the observed maximum; its CI ribbon is shown only within the observed range. ROV observations spanned the full range of unconsolidated substrate values, so ROV predictions (and CI ribbon) are shown across the full 0–100% substrate range.

Table 18. Predicted detection and occupancy validation results for pāku‘iku‘i at 153 NOAA CREP sites around Hawai‘i Island. Columns: site_id = CREP site identifier; logit_psi = model logit scale occupancy; psi_pred = back transformed occupancy probability ψ ; d1_uncon_z, d2_uncon_z = standardized percent unconsolidated substrate for divers 1 and 2; p_diver1, p_diver2 = predicted detection probabilities for each diver; psi_p_diver1, psi_p_diver2 = $\psi \times p$ for each diver; psi_p_any = probability of detecting at least one individual across both dives; observed_presence = observed pāku‘iku‘i presence (1) or absence (0) in the CREP data.

site_id	logit_psi	psi_pred	d1_uncon_z	d2_uncon_z	p_diver1	p_diver2	psi_p_diver1	psi_p_diver2	psi_p_any	observed_presence
H00094	0.50	0.62	-0.46	-0.41	0.52	0.48	0.32	0.30	0.52	1
H00111	0.22	0.56	-0.24	-0.41	0.35	0.48	0.19	0.27	0.41	0
H00153	0.28	0.57	0.08	-0.23	0.16	0.34	0.09	0.19	0.27	0
H00173	0.07	0.52	-0.42	-0.41	0.49	0.48	0.25	0.25	0.44	1
H00178	0.01	0.50	-0.58	0.11	0.62	0.15	0.31	0.07	0.36	0
H00181	0.08	0.52	-0.22	-0.55	0.34	0.59	0.17	0.31	0.43	1
H00190	0.09	0.52	0.28	-0.29	0.09	0.38	0.05	0.20	0.24	0
H00194	0.01	0.50	-0.13	-0.04	0.27	0.22	0.14	0.11	0.23	0
H00198	0.03	0.51	-0.48	-0.58	0.54	0.62	0.27	0.31	0.50	1
H00203	0.06	0.52	-0.27	-0.30	0.38	0.39	0.19	0.20	0.36	0
H00215	0.46	0.61	-0.08	-0.31	0.24	0.41	0.15	0.25	0.36	0
H00246	-0.06	0.49	0.11	-0.41	0.15	0.48	0.07	0.23	0.29	1
H00265	0.07	0.52	-0.24	-0.24	0.35	0.35	0.18	0.18	0.33	0

H00297	0.19	0.55	-0.49	-0.23	0.55	0.34	0.30	0.19	0.43	0
H00302	0.03	0.51	0.06	-0.32	0.17	0.41	0.09	0.21	0.28	0
H00323	-0.01	0.50	-0.41	-0.48	0.48	0.53	0.24	0.27	0.44	0
H00335	0.08	0.52	-0.58	-0.26	0.62	0.37	0.32	0.19	0.45	0
H00346	0.23	0.56	-0.41	-0.33	0.48	0.42	0.27	0.23	0.44	0
H00354	0.00	0.50	-0.58	-0.24	0.62	0.35	0.31	0.17	0.43	0
H00407	0.17	0.54	0.80	-0.24	0.02	0.35	0.01	0.19	0.20	0
H00416	0.24	0.56	-0.55	-0.41	0.59	0.48	0.33	0.27	0.51	0
H00430	0.10	0.52	-0.58	-0.58	0.62	0.62	0.32	0.32	0.54	1
H00431	0.13	0.53	0.46	0.63	0.05	0.03	0.03	0.02	0.05	0
H00433	0.14	0.54	-0.24	-0.06	0.35	0.23	0.19	0.13	0.29	0
H00447	-0.03	0.49	-0.58	-0.41	0.62	0.48	0.30	0.24	0.47	0
H00448	0.12	0.53	-0.41	-0.41	0.48	0.48	0.25	0.25	0.44	0
H00453	0.27	0.57	-0.31	0.39	0.40	0.07	0.23	0.04	0.25	0
H00460	0.24	0.56	-0.41	-0.41	0.48	0.48	0.27	0.27	0.46	0
H00468	0.17	0.54	-0.06	-0.24	0.23	0.35	0.13	0.19	0.29	0
H00469	0.32	0.58	0.11	-0.24	0.15	0.35	0.09	0.20	0.27	0

H00487	-0.04	0.49	-0.51	-0.41	0.56	0.48	0.28	0.24	0.45	0
H00488	0.11	0.53	0.11	0.80	0.15	0.02	0.08	0.01	0.09	0
H00503	0.26	0.56	-0.24	-0.01	0.35	0.20	0.20	0.12	0.29	0
H00526	-0.06	0.49	0.04	-0.58	0.18	0.62	0.09	0.30	0.36	0
H00532	0.24	0.56	-0.58	0.46	0.62	0.05	0.35	0.03	0.37	0
H00535	-0.09	0.48	-0.58	-0.41	0.62	0.48	0.29	0.23	0.45	0
H00549	0.17	0.54	-0.24	-0.41	0.35	0.48	0.19	0.26	0.40	0
H00582	0.35	0.59	-0.41	-0.41	0.48	0.48	0.28	0.28	0.48	0
H00583	0.43	0.61	-0.41	0.11	0.48	0.15	0.29	0.09	0.35	1
H00591	0.31	0.58	-0.58	-0.58	0.62	0.62	0.36	0.36	0.58	0
H00617	0.27	0.57	-0.51	-0.06	0.56	0.23	0.32	0.13	0.41	0
H00623	0.05	0.51	-0.58	-0.58	0.62	0.62	0.32	0.32	0.53	0
H00631	0.04	0.51	-0.06	-0.51	0.23	0.56	0.12	0.29	0.37	0
H00640	-0.05	0.49	-0.58	-0.58	0.62	0.62	0.30	0.30	0.51	0
H00643	-0.01	0.50	-0.58	-0.58	0.62	0.62	0.31	0.31	0.52	0
H00648	0.29	0.57	0.63	0.28	0.03	0.09	0.02	0.05	0.07	0
H00662	0.39	0.60	-0.41	-0.41	0.48	0.48	0.29	0.29	0.49	0

H00663	0.28	0.57	-0.58	-0.55	0.62	0.59	0.35	0.34	0.57	0
H00664	0.34	0.58	-0.58	-0.58	0.62	0.62	0.36	0.36	0.59	0
H00687	0.18	0.55	-0.55	-0.24	0.59	0.35	0.32	0.19	0.45	1
H00705	0.16	0.54	-0.58	-0.51	0.62	0.56	0.33	0.30	0.54	0
H00719	0.23	0.56	-0.58	-0.51	0.62	0.56	0.34	0.31	0.55	1
H00721	0.15	0.54	-0.58	-0.58	0.62	0.62	0.33	0.33	0.55	1
H00732	0.42	0.60	-0.58	-0.58	0.62	0.62	0.37	0.37	0.61	0
H00733	0.21	0.55	-0.51	0.11	0.56	0.15	0.31	0.08	0.37	0
H00735	0.19	0.55	-0.58	-0.58	0.62	0.62	0.34	0.34	0.56	1
H00750	0.38	0.59	-0.58	-0.58	0.62	0.62	0.37	0.37	0.60	0
H00754	0.35	0.59	-0.41	-0.41	0.48	0.48	0.28	0.28	0.48	0
H00755	0.37	0.59	-0.41	-0.06	0.48	0.23	0.28	0.14	0.38	1
H00757	0.47	0.62	-0.24	-0.24	0.35	0.35	0.21	0.21	0.38	1
H01773	0.19	0.55	0.11	-0.24	0.15	0.35	0.08	0.19	0.26	0
H01779	0.03	0.51	-0.41	0.63	0.48	0.03	0.24	0.02	0.26	0
H01785	-0.04	0.49	-0.10	0.04	0.25	0.18	0.12	0.09	0.20	0
H01798	-0.06	0.49	-0.34	-0.41	0.42	0.48	0.21	0.23	0.39	0

H01799	0.07	0.52	-0.41	-0.55	0.48	0.59	0.25	0.31	0.48	0
H01802	0.04	0.51	-0.06	0.28	0.23	0.09	0.12	0.05	0.16	0
H01807	0.00	0.50	-0.51	-0.24	0.56	0.35	0.28	0.17	0.41	0
H01824	0.14	0.54	-0.58	-0.58	0.62	0.62	0.33	0.33	0.55	0
H01825	0.02	0.51	-0.41	0.46	0.48	0.05	0.24	0.03	0.26	0
H01833	0.33	0.58	-0.41	-0.51	0.48	0.56	0.28	0.33	0.52	0
H01874	-0.03	0.49	-0.41	-0.34	0.48	0.42	0.24	0.21	0.40	0
H01887	0.24	0.56	0.11	-0.51	0.15	0.56	0.08	0.32	0.37	0
H01899	0.01	0.50	-0.06	-0.41	0.23	0.48	0.12	0.24	0.33	0
H01901	0.21	0.55	-0.51	-0.51	0.56	0.56	0.31	0.31	0.52	0
H01943	-0.11	0.47	0.63	-0.58	0.03	0.62	0.02	0.29	0.30	0
H01957	0.01	0.50	-0.41	0.11	0.48	0.15	0.24	0.07	0.30	0
H01960	0.00	0.50	0.63	0.63	0.03	0.03	0.02	0.02	0.03	0
H01985	0.02	0.50	0.28	-0.27	0.09	0.37	0.05	0.19	0.22	0
H01987	-0.06	0.48	-0.41	0.46	0.48	0.05	0.23	0.03	0.25	0
H01988	-0.03	0.49	-0.58	-0.55	0.62	0.59	0.30	0.29	0.51	0
H01994	0.03	0.51	-0.24	-0.24	0.35	0.35	0.18	0.18	0.32	0

H01999	0.23	0.56	0.11	-0.44	0.15	0.51	0.08	0.28	0.34	0
H02003	0.08	0.52	-0.24	-0.24	0.35	0.35	0.18	0.18	0.33	0
H02005	0.11	0.53	-0.41	-0.58	0.48	0.62	0.25	0.33	0.50	1
H02022	0.03	0.51	-0.06	0.46	0.23	0.05	0.12	0.03	0.14	1
H02032	-0.04	0.49	-0.41	1.15	0.48	0.01	0.24	0.00	0.24	0
H02034	0.34	0.58	0.28	0.63	0.09	0.03	0.05	0.02	0.07	0
H02063	0.02	0.50	-0.24	-0.24	0.35	0.35	0.17	0.17	0.32	0
H02075	0.06	0.51	0.11	1.15	0.15	0.01	0.08	0.00	0.08	0
H02090	0.13	0.53	-0.51	0.46	0.56	0.05	0.30	0.03	0.32	0
H02103	0.06	0.51	-0.41	-0.41	0.48	0.48	0.25	0.25	0.43	0
H02110	0.00	0.50	0.80	0.11	0.02	0.15	0.01	0.07	0.08	0
H02112	0.11	0.53	-0.55	-0.24	0.59	0.35	0.31	0.18	0.44	0
H02123	0.07	0.52	-0.58	-0.55	0.62	0.59	0.32	0.31	0.53	1
H02146	0.01	0.50	0.46	1.49	0.05	0.00	0.03	0.00	0.03	0
H02151	0.26	0.57	-0.58	-0.58	0.62	0.62	0.35	0.35	0.58	0
H02159	0.05	0.51	-0.41	-0.58	0.48	0.62	0.25	0.32	0.48	0
H02165	0.32	0.58	0.11	0.11	0.15	0.15	0.09	0.09	0.17	0

H02183	0.00	0.50	-0.24	-0.24	0.35	0.35	0.17	0.17	0.32	0
H02185	0.13	0.53	-0.24	-0.51	0.35	0.56	0.18	0.30	0.43	0
H02202	0.15	0.54	-0.58	-0.44	0.62	0.51	0.33	0.27	0.51	0
H02220	0.03	0.51	-0.41	-0.55	0.48	0.59	0.24	0.30	0.47	0
H02246	0.19	0.55	-0.48	0.28	0.53	0.09	0.29	0.05	0.33	0
H02248	-0.11	0.47	0.11	-0.51	0.15	0.56	0.07	0.27	0.32	0
H02259	0.01	0.50	0.11	-0.06	0.15	0.23	0.07	0.12	0.18	0
H02280	0.17	0.54	-0.24	-0.06	0.35	0.23	0.19	0.13	0.29	0
H02281	0.06	0.51	1.32	-0.06	0.00	0.23	0.00	0.12	0.12	0
H02290	0.07	0.52	-0.41	-0.48	0.48	0.53	0.25	0.28	0.46	0
H02306	0.06	0.51	0.28	0.11	0.09	0.15	0.05	0.08	0.12	0
H02315	0.10	0.53	-0.58	-0.41	0.62	0.48	0.32	0.25	0.49	0
H02318	0.04	0.51	-0.58	-0.41	0.62	0.48	0.31	0.24	0.48	1
H02348	0.01	0.50	0.46	-0.44	0.05	0.51	0.03	0.26	0.28	0
H02366	0.32	0.58	-0.48	-0.58	0.53	0.62	0.31	0.36	0.56	0
H02386	0.13	0.53	0.11	0.46	0.15	0.05	0.08	0.03	0.11	0
H02389	-0.08	0.48	-0.48	0.46	0.53	0.05	0.26	0.03	0.28	1

H02390	0.13	0.53	-0.24	-0.58	0.35	0.62	0.18	0.33	0.45	0
H02399	0.26	0.56	-0.48	-0.58	0.53	0.62	0.30	0.35	0.54	0
H02405	0.05	0.51	0.28	0.11	0.09	0.15	0.05	0.08	0.12	0
H02408	0.09	0.52	-0.58	-0.58	0.62	0.62	0.32	0.32	0.54	0
H02449	0.21	0.55	-0.31	-0.24	0.40	0.35	0.22	0.19	0.37	1
H02452	0.01	0.50	-0.24	-0.58	0.35	0.62	0.17	0.31	0.43	0
H02454	0.25	0.56	-0.58	-0.41	0.62	0.48	0.35	0.27	0.52	0
H02455	-0.03	0.49	-0.51	-0.58	0.56	0.62	0.28	0.30	0.50	1
H02465	0.06	0.51	-0.24	-0.41	0.35	0.48	0.18	0.25	0.38	1
H02467	0.03	0.51	-0.51	-0.48	0.56	0.53	0.28	0.27	0.48	0
H02468	0.17	0.54	0.11	0.46	0.15	0.05	0.08	0.03	0.11	0
H02524	-0.05	0.49	-0.58	-0.58	0.62	0.62	0.30	0.30	0.51	0
H02527	0.18	0.55	-0.58	-0.58	0.62	0.62	0.34	0.34	0.56	0
H02536	-0.20	0.45	-0.44	-0.51	0.51	0.56	0.23	0.25	0.42	0
H02597	0.23	0.56	-0.41	-0.31	0.48	0.40	0.27	0.22	0.43	0
H02618	0.46	0.61	-0.58	-0.58	0.62	0.62	0.38	0.38	0.61	0
H02626	0.04	0.51	-0.58	-0.55	0.62	0.59	0.31	0.30	0.52	1

H02711	0.25	0.56	-0.51	-0.24	0.56	0.35	0.32	0.19	0.45	0
H02733	0.17	0.54	-0.55	-0.55	0.59	0.59	0.32	0.32	0.54	1
H02762	0.29	0.57	-0.41	-0.48	0.48	0.53	0.27	0.31	0.50	0
H02771	0.32	0.58	-0.06	-0.41	0.23	0.48	0.14	0.28	0.38	0
H02777	0.20	0.55	-0.41	-0.44	0.48	0.51	0.26	0.28	0.47	0
H02786	0.08	0.52	-0.48	-0.48	0.53	0.53	0.28	0.28	0.48	1
H02787	0.13	0.53	-0.55	-0.44	0.59	0.51	0.31	0.27	0.50	1
H02792	0.07	0.52	0.28	-0.51	0.09	0.56	0.05	0.29	0.32	0
H02793	0.26	0.56	-0.24	-0.55	0.35	0.59	0.20	0.33	0.46	0
H02795	0.19	0.55	-0.48	-0.34	0.53	0.42	0.29	0.23	0.46	1
H02804	0.26	0.56	-0.58	-0.31	0.62	0.40	0.35	0.22	0.49	0
H02805	0.03	0.51	0.11	0.46	0.15	0.05	0.08	0.03	0.10	0
H02806	0.14	0.53	-0.06	0.11	0.23	0.15	0.12	0.08	0.19	1
H02821	0.35	0.59	-0.06	-0.24	0.23	0.35	0.14	0.20	0.31	0
H02824	0.08	0.52	-0.58	-0.41	0.62	0.48	0.32	0.25	0.49	1
H02826	0.44	0.61	0.11	-0.41	0.15	0.48	0.09	0.29	0.36	0
H02827	0.04	0.51	-0.41	-0.41	0.48	0.48	0.24	0.24	0.43	0

H02830	0.49	0.62	-0.34	-0.48	0.42	0.53	0.26	0.33	0.51	0
H02832	0.08	0.52	-0.48	-0.58	0.53	0.62	0.28	0.32	0.51	0
H02844	0.50	0.62	0.46	0.28	0.05	0.09	0.03	0.06	0.09	0
H02846	0.21	0.55	-0.48	-0.58	0.53	0.62	0.30	0.34	0.54	0

Table 19. Summary of predicted detection–occupancy probabilities ($P \geq 1$ detection) at sites where pāku‘iku‘i were either observed or absent in the NOAA Coral Reef Ecosystem Program (CREP) dataset. Values represent the number of sites (n), median predicted probability, and interquartile range (25th–75th percentiles).

Observed	n	Median	25th Percentile	75th Percentile
Absent	125	0.40	0.28	0.48
Present	28	0.48	0.38	0.52

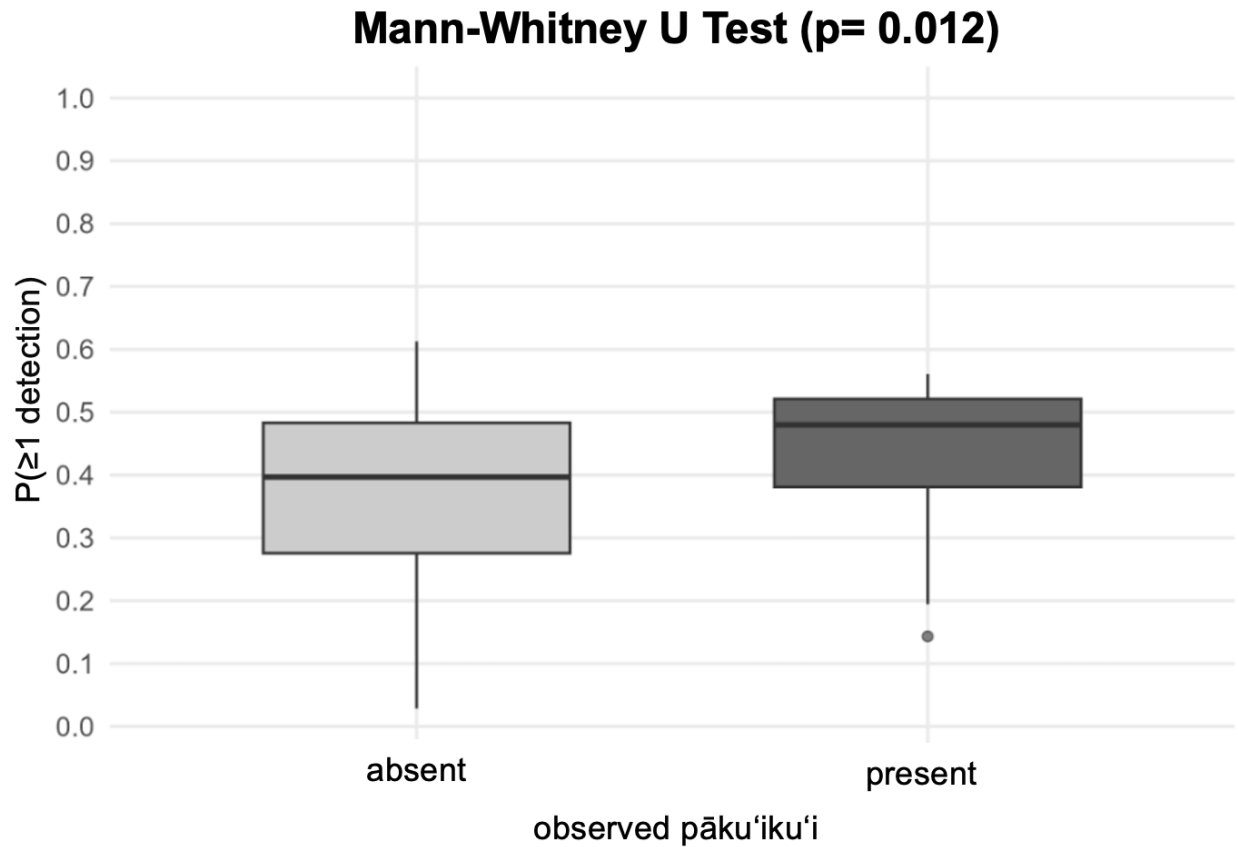


Figure 5. Comparison of predicted detection–occupancy probabilities ($P \geq 1$ detection) between sites where pāku'iku'i were observed and those where they were absent in the NOAA Coral Reef Ecosystem Program (CREP) dataset. Boxplots show medians, interquartile ranges, and outliers. A Mann–Whitney U test indicated that predicted probabilities were significantly higher at presence sites than absence sites ($W = 1218.0, p = 0.012$).

REFERENCES

- Ackerman J, Bellwood D (2000) Reef fish assemblages: A re-evaluation using enclosed rotenone stations. *Marine Ecology Progress Series* 206:227–237
- Adam TC, Schmitt RJ, Holbrook SJ, Brooks AJ, Edmunds PJ, Carpenter RC, Bernardi G (2011) Herbivory, connectivity, and ecosystem resilience: response of a coral reef to a large-scale perturbation. *PLoS ONE* 6:e23717
- Akaike H (1973) Information theory and an extension of maximum likelihood principle. In: Petrov BN, Csáki F (eds) *Proc Sec Int Symp Info Theory*. Akademia Kiado, Budapest, p 267-281
- Ali Abd Al-Hameed K (2022) Spearman’s correlation coefficient in statistical analysis. *Int J Nonlinear Analytical Appl* 13:3249–3255
- Andaloro F, Ferraro M, Mostarda E, Romeo T, Consoli P (2013) Assessing the suitability of a remotely operated vehicle (ROV) to study the fish community associated with offshore gas platforms in the Ionian Sea: a comparative analysis with underwater visual censuses (UVCs). *Helgol Mar Res* 67:241–250
- Anderson DR (2008) *Model based inference in the life sciences: a primer on evidence*. Springer, New York, NY
- Asner GP, Vaughn NR, Heckler JW (2020) *Global Airborne Observatory: Hawaiian Islands bathymetry 2019+2020 (Version 1.0)*. <https://doi.org/10.5281/zenodo.4294324> (accessed 2 April 2024)
- Asner GP, Vaughn NR, Heckler J (2020) *Global Airborne Observatory: Hawaiian Islands reef rugosity 2019+2020 (Version 1.0)*. <https://doi.org/10.5281/zenodo.4294332> (accessed 2 April 2024)
- Asner GP, Vaughn NR, Heckler JW (2022) *Global Airborne Observatory: Hawaiian Islands live coral cover 2020 (Version 1.0)*. <https://doi.org/10.5281/zenodo.4777345> (accessed 2 April 2024)
- Bacheler NM, Berrane DJ, Mitchell WA, Schobernd CM, Schobernd ZH, Teer BZ, Ballenger JC (2014) Environmental conditions and habitat characteristics influence trap and video detection probabilities for reef fish species. *Mar Ecol Prog Ser* 517:1–14
- Beijbom O, Edmunds PJ, Kline DI, Mitchell BG, Kriegman D (2012) Automated annotation of coral reef survey images. In: *Computer Vision and Pattern Recognition (CVPR), 2012 IEEE Conf*, 16–21 Jun 2012, Providence, RI. Curren Associates, Red Hook, NY, p 1170–1177
- Burnham KP, Anderson DR (2002) *Model selection and multimodel inference: a practical information-theoretic approach*. Springer, New York, NY

- Burnham KP, Anderson DR (2004) Multimodel inference: understanding AIC and BIC in model selection. *Sociol Methods Res* 33:261–304
- Cade BS (2015) Model averaging and muddled multimodel inferences. *Ecology* 96:2370–2382
- Coggins LG, Bacheler NM, Gwinn DC (2014) Occupancy models for monitoring marine fish: a bayesian hierarchical approach to model imperfect detection with a novel gear combination. *PLoS ONE* 9:e108302
- Friedlander AM, Brown EK, Jokiel PL, Smith WR, Rodgers KS (2003) Effects of habitat, wave exposure, and marine protected area status on coral reef fish assemblages in the Hawaiian archipelago. *Coral Reefs* 22:291–305
- Gilbert M, Rasmussen JB, Kramer DL (2005) Estimating the density and biomass of moray eels (Muraenidae) using a modified visual census method for hole-dwelling reef fauna. *Environ Biol Fishes* 73:415–426
- Grabowski TB, Masse R, McSwain D, Larson A, Raz LJ, Schemmel E, Bartz DE, Rodriguez N (2025) Age, growth, and reproductive biology of Achilles tang (*Acanthurus achilles*) around Hawai‘i Island, USA. *Environ Biol Fishes* 108:1–15
- Gray AE, Williams ID, Stamoulis KA, Boland RC, Lino KC, Hauk BB, Leonard JC, Rooney JJ, Asher JM, Lopes KH Jr, Kosaki RK (2016) Comparison of reef fish survey data gathered by open and closed circuit SCUBA divers reveals differences in areas with higher fishing pressure. *PLoS ONE* 11:e0167724
- Gretech Corporation (n.d.) GOM Player computer software. <https://www.gomlab.com/gomplayer-media-player/> (accessed 5 July 2024)
- Green SJ, Tamburello N, Miller SE, Akins JL, Côté IM (2013) Habitat complexity and fish size affect the detection of Indo-Pacific lionfish on invaded coral reefs. *Coral reefs* 32:413–421
- Harford WJ, Smith SG, Ault JS, Babcock EA (2016) Cross-shelf habitat occupancy probabilities for juvenile groupers in the Florida Keys coral reef ecosystem. *Mar Coast Fish* 8:147–159
- Hawai‘i Administrative Rule (HAR) §13-60.41 (2022) West Hawai‘i pāku‘iku‘i replenishment. Available from: <https://dlnr.hawaii.gov/dar/files/2022/12/ch60.41b.pdf> (accessed 20 September 2023)
- Hawai‘i Department of Land and Natural Resources, Division of Aquatic Resources (2019) Findings and recommendations of effectiveness of the West Hawai‘i Regional Fishery Management Area (WHRFMA). Report to the Thirtieth Legislature, 2020 Regular Session, in response to Section 188F-5, Hawai‘i Revised Statutes. Hawai‘i Department of Land and Natural Resources, Honolulu, HI
- Hawai‘i Statewide GIS Program (2022) County Council Districts – 2022. State of Hawai‘i, Office of Planning and Sustainable Development. <https://planning.hawaii.gov/gis/download-gis-data-expanded/> (accessed 20

September 2023)

- Heenan A, Williams ID, Acoba T, DesRochers A, Kosaki RK, Kanemura T, Nadon MO, Brainard RE (2017) Long-term monitoring of coral reef fish assemblages in the western central Pacific. *Sci Data* 4:1–12
- Hoover JP (2008) The ultimate guide to Hawaiian reef fishes, sea turtles, dolphins, whales, and seals. Mutual Publishing, Honolulu, HI
- Layko RB, Donovan MK (2024) Anthropogenic and environmental drivers of *Acanthurus achilles* presence in Hawai'i. *Mar Ecol Prog Ser* 740:161–174
- Lindfield SJ, Harvey ES, McIlwain JL, Halford AR (2014) Silent fish surveys: bubble-free diving highlights inaccuracies associated with SCUBA-based surveys in heavily fished areas. *Methods Ecol Evol* 5:1061–1069
- MacKenzie DI, Nichols JD, Lachman GB, Droege S, Royle JA, Langtimm CA (2002) Estimating site occupancy rates when detection probabilities are less than one. *Ecology* 83:2248–2255
- Mackenzie DI, Bailey LL, Nichols JD (2004) Investigating species co-occurrence patterns when species are detected imperfectly. *J Anim Ecol* 73:546–555
- MacKenzie DI (2006) Modeling the probability of resource use: the effect of, and dealing with, detecting a species imperfectly. *J Wildl Manag* 70:367–374
- MacKenzie DI, Hines J (2023) RPresence: R interface for Program PRESENCE. R package version 2.13.47. <https://www.usgs.gov/software/presence> (accessed 6 December 2024)
- MacNeil MA, Fonnesebeck CJ, McClanahan TR (2010) Occupancy models for estimating the size of reef fish communities. In: Riegl B, Dodge R (eds) Proceedings of the 11th International Coral Reef Symposium. National Coral Reef Institute, Nova Southeastern University, p 785–789
- Manley PN, Zielinski WJ, Schlesinger MD, Mori SR (2004) Evaluation of a multiple-species approach to monitoring species at the ecoregional scale. *Ecol Appl* 14:296–310
- Mann HB, Whitney DR (1947) On a test of whether one of two random variables is stochastically larger than the other. *Ann Math Stat* 18:50–60
- Mattfeldt SD, Grant EHC (2007) Are two methods better than one? Area constrained transects and leaf litterbags for sampling stream salamanders. *Herpetol Rev* 38:43–45
- McKann PC, Gray BR, Thogmartin WE (2013) Small sample bias in dynamic occupancy models. *J Wildl Manag* 77:172–180
- Meyer CG, Holland KN (2005) Movement patterns, home range size and habitat utilization of the bluespine unicornfish *Naso unicornis* (Acanthuridae) in a Hawaiian marine reserve.

- Meyer CG, Papastamatiou YP, Clark TB (2010) Differential movement patterns and site fidelity among trophic groups of reef fishes in a Hawaiian marine protected area. *Mar Biol* 157:1499–1511
- Nalmpanti M, Pardalou A, Tsikliras AC, Dimarchopoulou D (2021) Assessing fish communities in a multiple-use marine protected area using an underwater drone (Aegean Sea, Greece). *J Mar Biol Assoc U K* 101:1061–1071
- Nemeth M, Appeldoorn R (2009) The distribution of herbivorous coral reef fishes within fore-reef habitats: the role of depth, light and rugosity. *Caribb J Sci* 45: 247–253
- Nichols JD, Bailey LL, O’Connell AF, Talancy NW, Campbell Grant EH, Gilbert AT, Annand EM, Husband TP, Hines JE (2008) Multi-scale occupancy estimation and modelling using multiple detection methods. *J Appl Ecol* 45:1321–1329
- NOAA Coral Reef Ecosystem Program (CREP) (2025) National Coral Reef Monitoring Program dataset. Pacific Islands Fisheries Science Center, NOAA. <https://www.fisheries.noaa.gov/inport/item/28844> (accessed 20 September 2025)
- O’Connell AF, Talancy NW, Bailey LL, Sauer JR, Cook R, Gilbert AT (2006) Estimating site occupancy and detection probability parameters for meso- and large mammals in a coastal ecosystem. *J Wildl Manag* 70:1625–1633
- R Core Team (2025) R: a language and environment for statistical computing. R Foundation for Statistical Computing, Vienna. <https://www.R-project.org/>
- Randall JE (2001) Surgeonfishes of Hawai‘i and the world. Bishop Museum Press, Honolulu, HI
- Randall JE (2007) Reef and shore fishes of the Hawaiian Islands. Sea Grant College Program, University of Hawai‘i, Honolulu, HI
- Russ GR (2003) Grazer biomass correlates more strongly with production than with biomass of algal turfs on a coral reef. *Coral Reefs* 22:63–67
- Scharf FS, Manderson JP, Fabrizio MC (2006) The effects of seafloor habitat complexity on survival of juvenile fishes: species-specific interactions with structural refuge. *J Exp Mar Biol Ecol* 335: 167–176
- Schultz AL, Malcolm HA, Linklater M, Jordan AR, Ingleton T, Smith SD (2015) Sediment variability affects fish community structure in unconsolidated habitats of a subtropical marine park. *Mar Ecol Prog Ser* 532:213–226
- Schultz AL, Malcolm HA, Linklater M, Jordan AR, Ingleton T, Smith SD (2015) Sediment variability affects fish community structure in unconsolidated habitats of a subtropical marine park. *Mar Ecol Prog Ser* 532:213–226
- Sequeira AM, Mellin C, Lozano-Montes HM, Meeuwig JJ, Vanderklift MA, Haywood MD, Babcock RC, Caley MJ (2018) Challenges of transferring models of fish abundance between coral reefs. *PeerJ* 6:e4566

- Smith LL, Barichivich WJ, Staiger JS, Smith KG, Dodd CK (2006) Detection probabilities and site occupancy estimates for amphibians at Okefenokee National Wildlife Refuge. *Am Midl Nat* 155:149–161
- Stewart PS, Stephens PA, Hill RA, Whittingham MJ, Dawson W (2023) Model selection in occupancy models: inference versus prediction. *Ecology* 104:e3942
- Suarez B, Grabowski TB (2021)** Estimating detection and occupancy coefficients for the Pacific Islands coral reef fish species. Hawai‘i Cooperative Fishery Research Unit Technical Report Series HCFRU-001, University of Hawai‘i at Hilo, Hilo, HI.
<https://usgs-cru-individual-data.s3.amazonaws.com/t.grabowski/intellcont/HCFRU-001-1.pdf>
- Sward D, Monk J, Barrett N (2019) A systematic review of remotely operated vehicle surveys for visually assessing fish assemblages. *Front Mar Sci* 6:134
- Tissot BN, Hallacher LE (2003) Effects of aquarium collectors on coral reef fishes in Kona, Hawai‘i. *Conserv Biol* 17:1759–1768
- Vergés A, Vanderklift MA, Doropoulos C, Hyndes GA (2011) Spatial patterns in herbivory on a coral reef are influenced by structural complexity but not by algal traits. *PLoS One* 6:e17115.
- Wedding LM, Lecky J, Gove JM, Walecka HR, Donovan MK, Williams GJ, Jouffray JB, Crowder LB, Erickson A, Falinski K, Friedlander AM (2018) Advancing the integration of spatial data to map human and natural drivers on coral reefs. *PLoS ONE* 13:e0189792
- Wilcoxon F (1945) Individual comparisons by ranking methods. *Biom Bull* 1:80–83
- Williams ID, Walsh WJ, Tissot BN, Hallacher LE (2006) Impact of observers’ experience level on counts of fishes in underwater visual surveys. *Mar Ecol Prog Ser* 310:185–191
- Willis T (2001) Visual census methods underestimate density and diversity of cryptic reef fishes. *J Fish Biol* 59:1408–1411